11-17-2008

# Role of MAP Kinase in Fusarium Association With Contact Lenses

Brook Alicia Danboise

# THE ROLE OF MAP KINASE IN *FUSARIUM* ASSOCIATION WITH CONTACT LENSES

by

BROOK ALICIA DANBOISE

Under the Direction of Dr. Sidney A. Crow, Jr.

## ABSTRACT

*Fusarium solani* is a soil-borne pathogen devastating agricultural crops throughout the world. While most pathogens are host specific, the fusaria are able to infect both plants and animals. In 2004, an outbreak of *Fusarium* occurred in association with contact lens wear. Several species of *Fusarium* were involved but *F. solani* and *F. oxysporum* were most prominent. In this work, we have identified a MAP kinase (MAPK), highly similar to *fmk1* in *F. oxysporum,* belonging to the YERK1 subfamily of extracellular regulated kinases. Directed disruption of *fmk1* in *F. solani* AFR4 (FSSC 1) affected several aspects of fungal growth and pathogenicity. Colonies of AFR4$\triangle$*fmk1* displayed pigmented colony-like formation as opposed to the cottony-white diffuse growth observed with the wild-type strain. Mutants displayed changes in morphology and conidiation patterns with AFR4$\triangle$*fmk1* mutants producing increased amounts of macroconidia vs. microconidia. AFR4$\triangle$*fmk1* germ tube emergence was similar to

that of wild-type AFR4 and wet weight growth was equivalent but germinules were not able to sense nutrient in chemotropic assays. The disruption of *fmk1* increased spore surface hydrophobicity leading to a decrease in association with commercially available hydrogel contact lenses. FMK1 did not affect unworn lens penetration in phosphate buffered saline as both wild-type and mutant strains were able to penetrate commercially available silicone hydrogel contact lenses. AFR4 displayed increased penetration of silicone lenses and this is likely due to: increased spore/lens association, and the inability of AFR4△*fmk1* macroconidia to germinate in phosphate buffered saline. Diminished invasive growth was also noted with disruption of *fmk1*. Wild-type AFR4 was detected throughout the eye after conidial microinjection while AFR4△*fmk1* was limited to the vitreous fluid. The reduced invasive growth seen is attributed to the loss of chemotropism. The ability to sense and respond to the environment is essential for pathogenicity. MAPK has been deemed essential for plant pathogenicity and now, with its affect on chemotropism, appears to be necessary for animal pathogenicity. FMK1 plays a conserved role in the pathogenicity of *Fusarium*.

INDEX WORDS: *Fusarium solani*, MAP kinase, Contact lens, Mycosis, *Fusarium* keratitis

# THE ROLE OF MAP KINASE IN *FUSARIUM* ASSOCIATION WITH CONTACT LENSES

by

BROOK ALICIA DANBOISE

A Dissertation Submitted in Partial Fulfillment of the Requirements for the Degree of

Doctor of Philosophy

in the College of Arts and Sciences

Georgia State University

2008

THE ROLE OF MAP KINASE IN *FUSARIUM* ASSOCIATION WITH CONTACT LENSES

by

BROOK ALICIA DANBOISE

Committee Chair: Sidney A. Crow, Jr.

Committee: George E. Pierce
Robert B.Simmons

Electronic Version Approved:

Office of Graduate Studies
College of Arts and Sciences
Georgia State University
December 2008

# DEDICATION

I dedicate this work to my family:

My mom, Rosie MacDonald, who was ever enthusiastic and encouraging.

My dad, David Danboise, who always knew I could do it.

Wes MacDonald, second dad extraordinaire, need I say more.

And my husband, Keith Forehand, who was more patient and supportive than could have (or should have) been expected.

I couldn't have done it you. Please except this small token of my love and gratitude.

# ACKNOWLEDGEMENTS

This dissertation has been a journey and there are many, many people I owe thanks to for providing guidance along the way. First, I have to thank my advisor, Dr. Sidney Crow for providing me with the opportunity to find my way. His encouragement and enthusiasm allowed me to combine the dark side of microbiology with molecular to produce this dissertation. I would also like to thank Dr. George Pierce and Dr. Robert Simmons for their support during this project. Dr. Gladys Alexandre was an amazing mentor, who introduced me to molecular biology, and for that I am grateful. Dr. Trudy Tucker, Dr. Sam Demons, Dr. Anthony Jones, and Dr. Bonnie Stephens provided brilliant contributions to this project and kept me focused while Ginger Moulder, Mara Maroney and Hollis Walker contributed friendship and support. Thank you all.

TABLE OF CONTENTS

# LIST OF TABLES

# LIST OF FIGURES

## I. INTRODUCTION

*Fusarium* is a filamentous fungus belonging to the family Hypocreaceae (6). *Fusarium* species are ubiquitous within soils and decimate crop plants such as cotton, watermelon, potato, tomato, and grasses. Since they are responsible for wilt, blight, canker, and root rot of crop plants and trees, *Fusarium spp*. are of great agricultural and economical importance. *Fusarium* was first described in the 16$^{th}$ century as a pathogen of maize. As *Fusarium* continued to be problematic during the growth and storage of crops, it was further studied yielding the first species description by Link in 1809 (6). Further species description has continued over the centuries with over 1,000 species defined at one time and a debatable number of species defined to date (38).

*Fusarium* species are generally identified by their unique morphology. They may produce macroconidia, microconidia and chlamydospores. The hyphae are generally described as septate and hyaline, and the macroconidia are septate and fusiform with a thick wall. The macroscopic growth of these fungi tends to vary depending on the growth conditions and medium employed, often making differentiation between species difficult. Recently, several sequence-based methods have been used to identify fungal genera and species. The sequence-based methods have decreased identification error as well as the time required to properly identify fungal genera and species (39).

*Fusarium* species are not only plant pathogens, but are also pathogenic to humans and animals. *Fusarium* was first suggested to be infectious in humans in 1916 when Greco published "The origin of tumours" in which *Fusarium* was described as the causative agent of a nasal fungal infection (6). *Fusarium* species were originally thought to be associated with either disease in humans or disease in plants. It is now apparent that the mechanism of infection for

animals and plants is conserved, allowing one species to cause pathogenesis in multiple hosts (41, 56). Fungal infections are most often seen in the immunocompromised, the immunosuppressed, and contact lens wearers.

Contact lenses are most commonly employed in vision correction, but are also employed as therapeutic agents and used cosmetically. Modern contact lenses can be safely used with few side-effects, when use and care instructions are followed properly. Recently, mycoses, such as *Fusarium* keratitis, have been linked to improper care and use of contact lenses (11, 57).

**History of Contact Lenses**

Contact lenses were first conceived by Leonardo da Vinci in *Codex of the Eye*, in 1508; however, the first glass lens was not produced until 1887 (22). The original glass lenses were large, covering the entire eye, and could only be worn for short durations because gas did not permeate the lens. In 1939, plastic lenses were developed. These lenses were lighter than the glass lenses, but continued to cover the entire eye making them difficult to use. In 1948, plastic lenses were designed that covered only the cornea. These lenses were easier to use, but still did not allow gas to permeate the lens. The 1970's brought about two advances in contact lenses: oxygen permeable lenses and soft contact lenses (33). Today there are a number of disposable soft contact lenses commercially available for both cosmetic and vision correction purposes.

Advances in contact lens design lead to the production of soft hydrogel lenses. The hydrogel lens contains an increased amount of water, but the polymer material still does not transmit large amounts of oxygen to the eye. In the late 1990's the need for increased oxygen transmission lead to the development of silicone hydrogel contact lenses. The addition of silicone increased not only the oxygen permeability of the lens, but also the hydrophobic

potential of the lens (53). Today, silicone hydrogel contact lenses account for 45% of all lenses sold.

Hydrogel lenses, whether silicone or typical hydrogel lenses, vary greatly from manufacturer to manufacturer. Table 1 depicts the various materials used to manufacture commercially available hydrogel lenses, while Table 2 depicts the materials used in production of silicone hydrogel lenses. Also included in Table 2 is the post-production surface treatment or internal wetting agent polyvinylpyrrolydone (PVP) required in the manufacturing process. Lenses manufactured by different industries vary in material, pore size, and surface treatment of the lens. Changes to any of these characteristics change the behavior of the lens in relation to sorption and molecular transport (28).

Table 1: Commercially available hydrogel contact lenses Adapted from Jones *et al*. (28)

| **Commercial name** | **Manufacturer** | **Common Name** |
|---|---|---|
| Frequency 38 | CooperVision | polymacon |
| Optima FW | Bausch & Lomb | polymacon |
| Preference | CooperVision | tetrafilcon |
| Biomedics 55 | Ocular Sciences | ocufilcon D |
| Focus (1-2 wks) | CIBA Vision | vifilcon |
| 1-Day Acuvue | Vistakon | etafilcon |
| Acuvue 2 | Vistakon | etafilcon |
| Proclear Compatibles | CooperVision | omafilcon |
| Soflens 66 | Bausch & Lomb | alphafilcon |
| Focus Dailies | CIBA Vision | nelfilcon |
| Soflens One Day | Bausch & Lomb | hilafilcon |
| Precision UV | CIBA Vision | vasurfilcon |

Table 2: Commercially available silicone hydrogel contact lenses including common name and surface treatment used in manufacturing Adapted from Jones *et al.* (28)

| Commercial name | Manufacturer | Common Name | Surface Treatment |
|---|---|---|---|
| PureVision | Baush & Lomb | balafilcon A | Plasma Oxidation |
| Focus Night & Day | CIBA Vision | lotrafilcon A | Plasma Coating |
| Acuvue Advance | Vistakon | galyfilcon A | None (PVP wetting agent) |

**Fusarium as a Human Pathogen**

*Fusarium* was first noted as an opportunistic human pathogen in the 20th century. As antibiotic use gained momentum in the 1940's and steroid use in the 1950's, the number of *Fusarium* related mycoses increased (6). *Fusarium* has typically been described as a plant pathogen, but with an increase of immunocompromised individuals and increases in contact lens wear, the occurrences of *Fusarium* mycoses are rising. In 1984, there were only 200 recorded cases of *Fusarium* mycosis, while in May 2006, there were over 100 cases of *Fusarium* related keratitis diagnosed that year in the U.S. alone (3, 10). Previously, *Fusarium* associated keratitis was linked with trauma to the eye, but today, fungal infection accounts for 1% of all contact-lens related microbial keratitis, and 30% of all *Fusarium* keratitis is associated with contact lens wear (18, 47).

**Outbreak of *Fusarium***

Contact lens associated keratitis is usually caused by bacteria, most notably *Pseudomonas aeruginosa* (29). Bacterial keratitis is increased in contact lens wearers over incidence in the

general populace. Bacteria attach to the lens forming biofilms. These biofilms make organisms more resistant to disinfection, allowing them to persist on the lens (55). Biofilms can consist of bacterial and/or fungal species.

Five in one million contact lens wearers contract *Fusarium* associated keratitis annually, but between 2004 to 2006, there was an outbreak of *Fusarium* keratitis associated with contact lens wear (52). The *Fusarium* outbreak has been linked to the use of certain contact lens solutions and improper lens care. By May of 2006, there were 102 cases of *Fusarium* keratitis reported in the United States (10). A month later, in June 2006, the number of diagnosed cases of *Fusarium* keratitis had risen to 164 cases in the US (11, 29).

Subtropical climates such as Singapore and Florida have increased incidence of *Fusarium* keratitis. From 2000-2004 there were 3 cases of contact lens related *Fusarium* keratitis diagnosed in Singapore. In late 2005, an increase in cases justified inquiry into the cause. A total of 66 cases of *Fusarium* keratitis were identified in Singapore by culture of corneal scrapings. Of those 66 cases, 15 were genotyped using a 28s rRNA marker. All of these cases were identified as *F. solani* CBS 490.63. Patient lenses, lens cases, and solutions were collected when available. Ten bottles of solution were tested for microbial contamination; none were *Fusarium* contaminated. Interviews with patients conducted during the course of the study revealed poor lens hygiene. During the course of inquiry it was also revealed that <93% of patients had used a Bosch and Lomb ReNu product for disinfection (29).

In 2006, several cases of *Fusarium* keratitis were identified by the CDC in the United States. By the end of the outbreak >150 patients had been identified with *Fusarium* keratitis in the US. The used lenses, lens cases, and lens solutions were collected from these patients when available and tested for contamination. The liquids in solution bottles were filtered and cultured

to identify contaminating organisms, but none were found. Lens cases and open solution bottle tops were swabbed and cultured. Two solution bottle caps of 26 patient-submitted bottles tested, showed *Fusarium* contamination, while 6 of 11 used contact lenses with cases showed contamination. None of the unopened lenses, solutions, or cases was *Fusarium* contaminated. The lack of contamination of unused lenses and products suggested that contamination was likely due to patient transfer from the environment and possible deviation from lens care guidelines (11, 57). The recent outbreak of *Fusarium* keratitis demonstrates the consequence of *Fusarium* as an opportunistic pathogen associated with contact lens wear.

**Molecular Identification of *Fusarium***

Currently, there are several methods available for the molecular identification of *Fusarium*. The most commonly used molecular technique for the identification of *Fusarium* is a sequence-based technique. The sequence-based approach to identification involves the amplification of a portion of a target gene. The amplified portion of the target gene is sequenced and compared to a database, either BLAST (http://www.ncbi.nlm.nig.gov/BLAST/ ) or Fusarium-ID v. 1.0 (http://fusarium.cbio.psu.edu/), yielding a probable identification (19).

Several target genes have been suggested for use in the molecular identification of fungi. The genes targets currently being utilized include, but are not limited to: the 18s and 28s rRNA genes, the internal transcribed spacer region (ITS) of the rRNA operon, and the intergenic spacer region (IGS) of the rRNA operon, as well as the translation elongation factor alpha (TEF) (9, 16, 17, 21, 23, 25, 26, 36, 39, 51, 54). Figure 1 depicts the fungal rRNA operon including the IGS region, the ITS region, the 18s and 28s rRNA gene regions (16).

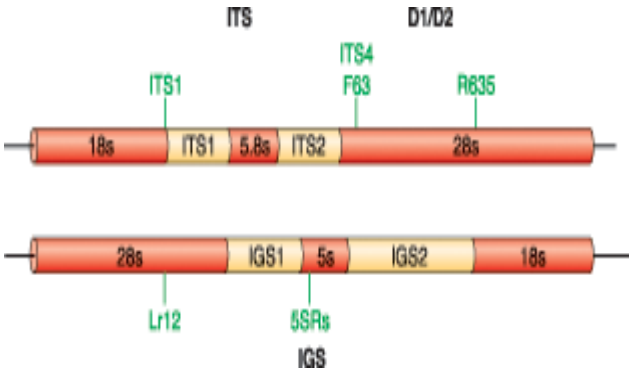


Figure 1: Organization of the fungal rRNA operon depicting the 18s, 28s, ITS, and IGS regions. Diaz, M. 2006. Microbe. 2: 74-81.

In choosing a gene for the identification of fungi, it is best to utilize an intron-rich sequence. The quickly evolving intron-rich regions often allow for fungal speciation with the use of a lone DNA locus. The rRNA operon and the TEF region are currently the most popular choices for fungal identification due to the large amount of both conserved and non-conserved regions in these loci (16, 19). The β-tubulin allele is less commonly used for identification, but has been shown to speciate *Fusarium* isolates (20). β-tubulin has also been used in absolute quantification of *Fusarium graminearum* in plants (44). The highly divergent nature of this allele within *Fusarium* allows for its use in speciation as well as in quantification (40).

**Challenge Assay**

Recently, various studies have been undertaken to determine the effectiveness of contact lens disinfectant solutions. The basic design of these assays is to use plate counts to determine the effectiveness of a disinfectant solution in reducing the microbial load of a contact lens incubated with fungi. First, a lens is incubated with an inoculum for a given amount of time.

Next, the lens is transferred to a volume of commercially available lens disinfectant and incubated for 10 minutes to 4 days. The lens or the solution is then plated on various media and incubated for up to two weeks. The colonies are counted to determine the ability of the solution to reduce the microbial load, and if multiple organisms were used as inoculum, then morphological characteristics are used to determine the population composition of the surviving community (37, 57). The challenge assay described above, while effective, is time demanding and subject to investigator bias. It can be improved upon with molecular techniques.

Molecular techniques can improve the quality, as well as the quantity, of information provided in a challenge assay. In the current challenge assay, genus/species identification is based on morphological characteristics and pigments of the fungi. These characteristics can take up to two weeks to fully develop and vary depending on the type of media and conditions of cultivation (39). With sequencing techniques, the genus/species identification can be done in as little as 24 hours, without the bias that can occur with morphology-based identifications. Also, with the current assay, if quantification of fungi associated with a contact lens is necessary, plate counts must be performed. Plate counts can prove problematic due to the fact that many plates become overgrown before morphological characteristics are well developed and can be analyzed to determine genus and/or species. Flow cytometry can also be used for quantification, but often detection requires over 10,000 cells/conidia per sample. With the development of real-time PCR, it is now possible to detect and quantify between 1-100 organisms (26, 51). The real-time PCR protocol should exceed the efficiency of traditional methods for the detection and quantification of active fungal species.

The use of molecular methods can aid the research process for contact lens associated fungi, including *Fusarium*. The use of sequence-based techniques decreases the time required

for genus and species identification and also eliminates bias that can be introduced using morphology-based identification. With the use of real-time PCR, the number of contact lens associated *Fusarium* can be detected and quantified in hours vs. days or weeks.

**Quantitative Real -Time PCR**

Recently, methods for determination of fungal burden in plant and animal tissues have been described. These methods rely on quantitative real-time PCR. Quantitative real-time PCR, the most sensitive technique currently available, allows quantitation of as little as one conidial equivalent (CE) from a relatively small starting sample. This technique utilizes either a sequence-specific fluorescent probe, such as TaqMan® (Ambion, Austin, TX.) or a SYBR® green dye.

SYBR® green dye is the most economical and most undemanding chemistry used in quantitative real-time PCR. SYBR® green intercalates in dsDNA and fluoresces green when illuminated with blue light (Ab 458, Em 522 μm). Therefore, as the amount of PCR product (dsDNA) increases, the amount of fluorescence increases allowing for quantitation. The downfall of using SYBR® green vs. a TaqMan® probe is that SYBR® green will adhere to any DNA while the TaqMan® probe is sequence specific (13).

A standard, utilizing serial dilutions from samples of known copy number, must be generated within each assay to allow for the quantification of transcript number or microbial load in an unknown sample. The $\triangle$Rn is the fraction of the fluorescent signal at a time point, while the Ct value is the cycle number at which the fluorescence detected is above background. PCR cycle number vs. $\triangle$Rn of the reaction is plotted to yield a Ct value for each sample. By

comparing the unknown Ct values to the Ct values of known molecular numbers, the absolute quantification of the gene or organism in the sample is able to be determined (9, 13, 49).

Quantitative real-time PCR lends itself well to the detection of contact lens associated fungi, including *Fusarium*. By targeting single copy, variable regions of the genome, such as the ITS or β-tubulin genes, primers specific for *Fusarium* can be designed for use in quantification of contact lens associated *Fusarium*. Quantitative real-time PCR allows for the rapid detection and quantification of fungal samples from small sample volumes (7).

**MAP Kinase**

Mitogen-activated protein (MAP) kinases (MAPK) are highly conserved in eukaryotic systems. They are activated by a mitogen, or extracellular signal, that is converted to an intracellular response. MAP kinase is universally activated but yields a specific response due to the specificity of phosphorylation during the cascade (50). As shown in figure 2, the MAP kinase cascade consists of an extracellular stimulus, MAP kinase kinase kinase (MAPKKK), MAP kinase kinase (MAPKK), MAPK and response in transcription control (31, 34). MAP kinases are serine/threonine specific kinases with MAPKK phosphorylating MAPK and MAPKKK activating MAPKK. There are often several MAPK pathways in eukaryotic cells, each being distinct and involving a unique response in gene transcription (50). MAPK signal transduction cascades are essential in sensing environmental conditions and regulating gene transcriptions. Cell differentiation, cell death, and cell growth are all dependent on the MAPK signal transduction cascade. Without the cascade an organism is less able to sense and therefore, adapt to its environment (30).

MAP kinase cascades regulate virulence in plants. Virulence is composed of recognition, attachment, and penetration of the host and likely relies on a conserved signal transduction cascade involving MAPK. In *Colletotrichum,* deletion of MAPKK leads to a loss of appressorium, a virulence structure, production decreasing the infectious ability of the fungi (30). In *F. oxysporum*, deletion of MAPK leads to changes in plant virulence. MAP kinase deletion decreases surface hydrophobicity, as well as invasive growth. Penetration hyphae are absent in MAPK mutants as well leading to an overall decrease in virulence. In *Fusarium*, MAPK is encoded for by *fmk1*. The role of *fmk1* in contact lens attachment and penetration is currently unknown. In *Fusarium, fmk1* plays a crucial role in attachment and penetration of stem and root structures of plants (14).

**The *Fusarium solani* Species Complex**

The *Fusarium solani* species complex (FSSC) has been generated using multilocus haplotyping. The loci used in the haplotyping include: the translation elongation factor (TEF 1-$\alpha$), the internal transcribed spacer (ITS) region, and a portion of the large subunit (LSU) of the rRNA gene. The haplotyping divided the FSSC into 3 clades with all species associated with human infection residing within clade 3. Within the FSSC there are 18 distinct species pathogenic to humans. These 18 species are infectious not only in humans but also in plants and widely distributed in the environment (56).

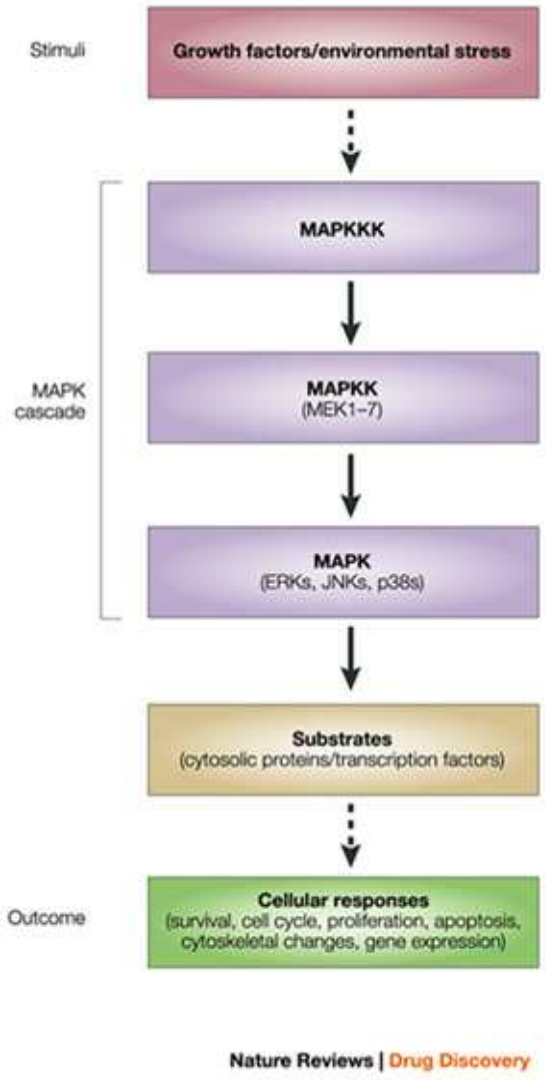


Figure 2: Example of a generic MAP kinase cascade. Kumar, S.2003. Nat. Rev. Drug Discov.2: 717-26.

**Rationale**

*Fusarium* is a well characterized plant pathogen that has recently been recognized for its ability to cause infection in humans. With an increase in the populations of immune

compromised persons and contact lens wearers has come an increase in the occurrences of *Fusarium* mycoses. In 2006, an outbreak of *Fusarium* keratitis was associated with contact lens wear. With an increase of infection comes the need for unbiased, reliable methods for identification, quantitation, and speciation of *Fusarium* species. It is one intent of this work to develop a method for the quantitation of *Fusarium* from contact lenses using real-time PCR absolute quantification techniques. The quantitation techniques developed could ultimately be applied to improve current challenge assay strategies.

Recently there has been an effort to haplotype *Fusarium,* defining distinct species and further breaking them into clades to predict infectious potential. This work has resulted in creation of the *Fusarium solani* species complex (FSSC) as well as the *Fusarium oxysporum* species complex (FOSC). Within each complex, a group of potentially human pathogenic *Fusarium* has been noted. These distinctions are based on relationships between structural genes of known human pathogens; these distinctions are not based on a marker associated with fungal pathogenicity. A second objective of this work is to ascertain the role of MAP kinase in *Fusarium* association with contact lenses.

## II. MATERIALS AND METHODS

### Materials and Bacterial Strains

All chemicals used during this study were obtained from Sigma (St. Louis, MO) or Difco (BD, Franklin Lakes, NJ). Plasmids were maintained in *Escherichia coli* JM109 cells (Promega, Madison, WI). Restriction, as well as modification, enzymes were purchased from NEB (Ipswich, MA).

### Fungal and Culture Conditions

Cultures of *Fusarium oxysporum* strain AFR9 and *Fusarium solani* strain AFR4 were graciously provided by Dr. Donald Ahearn, Georgia State University. *Fusarium* cultures were routinely grown on Potato Dextrose Agar (PDA) for 3-5 days at room temperature. Conidia were harvested and resuspended per the method of Crow et al (45).

Table 3: Primers used in this study

| Primer Name | Sequence | Reference |
|---|---|---|
| PFFOR | 5' AGG GAT GTA TTT ATT AGA TAA AAA ATC AA | JAEGER, E |
| PFREV2 | 5' CGC AGT ACT TAG TCT TCA GTA AAT C | JAEGER, E |
| BTUB1 | 5' TAC TTC GTC GAG TGG ATT CC | YAN |
| BTUB2 | 5' TGG TAC TGC TGG TAC TC | YAN |
| AFRBTF | 5' TCG ATC TTG AGC CTG GTA CCA | This study |
| AFRBTR | 5' GTT TCC AGC ACC CCA CTG A | This study |
| OLIFMK1 | 5' ATG TCC CGA TCG AAC CCC CC | DIPIETRO |
| OLIFMK2 | 5' CTG TTA CCT CAT AAT CTC CTG G | DIPIETRO |
| AFR18SF | 5' CTG CTG CCT TCC TTG GAT GTA G | This study |
| AFR18SR | 5' GGG TAT TGG CCA AAC ATG GTT | This study |

**"Eye" Model for Fungal Penetration**

A Coors 12-well ceramic watch glass (model 60429) was used to model the shape of the eye. To create the "eyes", molten PDA was dispensed into each well of the watch glass and allowed to cool. "Eyes" were removed to sterile Petri plates and covered with silicone hydrogel contact lenses. The lenses were inoculated with 10 µl *F. oxysporum* AFR 9 conidial suspension ($10^7$/conidia $ml^{-1}$) and incubated at room temperature for 24-48 hours. Control samples were grown in potato dextrose broth (PDB).

**Sonication of "Eyes" for Protein Extraction**

After 24-48 hours of incubation, the lenses were removed from the "eyes". Lenses were rinsed in sterile phosphate buffered saline (PBS) and transferred to 15 ml conical bottom tubes. The lenses were covered with lysis buffer (30 mM Tris, 7 M Urea, 2 M Thiourea, 4% Chaps) and sonicated 5 minutes with cycling of 5 seconds on, 10 seconds off. Protein was then concentrated using trichloroacetic acid and quantitated.

**SDS-PAGE**

Samples were prepared for sodium dodecyl polyacrylamide gel electrophoresis by boiling of the samples for 10 minutes in 2X sample buffer (50 mM Tris-HCl, pH 6.8; 10% glycerol; 2% SDS; 5% β-mercaptoethanol; 0.1% bromophenol blue). Samples were loaded onto 12% gels with Amersham protein molecular weight marker. Staining was done according to the modified silver staining protocol of Blum (43). Briefly the gels were fixed in 40% EtOH, 10% HAc overnight,and then washed in 30% EtOH followed by washing in $dH_2O$. Sensitizing was done in

0.02% $Na_2S_2O_3$ for 1 minute and gels were then washed in $dH_2O$. Gels were then placed at 4°C in 0.1% $AgNO_3$ for 20 minutes then rinsed again in $dH_2O$. The gels were developed in 3% $Na_2CO_3$, 0.05% formalin until color change was sufficient. Staining was terminated with 5% HAc and the gels were stored at 4°C in 1% HAc. Bands unique to the attached AFR9 samples were selected, excised, and sent to the Georgia State University Core Facility (Atlanta,GA) for digestion, concentration and MALDI-TOF-TOF analysis.

**DNA Extraction**

Conidia were placed into a 2 ml screw-cap tube with 500 mg, 0.5 mm glass beads (Biospec Products, Bartlesville, OK). Samples were processed in a Bead Beater (Biospec Products, Bartlesville, OK) at 4800 rpm for 30 seconds, three times with tubes held on ice between bashings. 600 µl cold phenol:chloroform:isoamyl alcohol (25:24:1) was added to the sample, and the tubes were vortexed for one minute followed by centrifugation for 10 minutes at 14,000 rpm, 4°C. The aqueous phase was transferred to a new tube and 1/10 the volume sodium acetate and 2 volumes absolute ethanol were added. DNA was precipitated for one hour on ice and collected by centrifugation for 30 minutes at 14000 rpm, 4°C. DNA was washed in 70% ethanol and resuspended in nuclease-free $dH_2O$ (Fermentas, Glen Burnie, Maryland).

**DNA Extraction From a Contact Lens**

For the isolation of DNA from contact lenses, the protocol above was modified as follows. One lens with attached fusaria was added to a 2 ml screw-cap tube with 500mg, 0.5 mm glass beads. One ml of saline was added to the tube, and extraction proceeded as previously

described. Samples were resuspended in 10 µl nuclease-free $dH_2O$ and stored at –20°C for future use.

**Determination of Extraction Efficiency**

Extraction efficiency was determined using known numbers of *F. oxysporum* conidia ranging from 10 to$10^5$ conidia. For this assessment, a known number of conidia resuspended in saline and a naïve contact lens were added to a 2 ml screw-top vial. DNA was extracted from the conidia / naïve lens according to the protocol for DNA extraction from a contact lens. Each concentration was used as the template in a qPCR reaction to determine the number of conidial equivalents. The number of CE determined from the qPCR reaction was adjusted to account for the dilution of the reaction and compared to the number of conidia from the initial extraction. Comparison of known number of conidia to CE determined percent DNA extraction efficiency.

**Primer Design**

Primers were designed to target a 101 base pair region of the *Fusarium* 18s gene to be used in real-time PCR, as well as a 102 base pair region of the β-tubulin gene. For development of the primer sets, genomic DNA was isolated from *F. oxysporum* AFR9 and *F. solani* AFR4. Primers PFFOR and PFREV2 were used to amplify a 1 kb region of the gene 18s gene and primers BTUB1 and BTUB2 were used to amplify a 400 bp region of the β-tublin gene from each strain. Amplicons were sequenced by the Georgia State University Core Facility and aligned utilizing BioEdit software. Conserved sequences were identified and primers for each gene were designed from conserved regions of the AFR9 and AFR4 aligned sequences.

**Quantitative PCR Reaction**

The qPCR reaction utilized Power SYBR® Green PCR Master Mix (Applied Biosystems, Foster City, CA) in a 25µl total volume with 900 nM each primer (AFRBTF/R or AFR18SF/R) with 2 µl template DNA. Cycling parameters consisted of an initial denaturation at 50°C for 2 minutes then 95°C for 10 minutes followed by 40 cycles of: 95°C 15 seconds, 60°C 1 minute. A dissociation step followed the completed run with 95°C 15 seconds, 60°C 1 minute, and 95°C 15 seconds. The qPCR was done in an Applied Biosystem 7500 (Applied Biosystems, Foster City, CA) Georgia State University Core Facitity and the data was analyzed using SDS software from Applied Biosystems.

**Standard Curve for qPCR**

A standard curve was generated to determine the range of accuracy for copy number detection. To create the standard curve, primer sets AFRBTF/AFRBTR and AFR18SF/AFR18SR were used to amplify an ~100 bp target from AFR4 genomic DNA. Each amplicon was visualized by gel electrophoresis and purified using a Qiagen PCR PURE kit (Qiagen, Valencia, CA). The concentration of product was determined spectrophotomically using an Eppendorf Biophotometer (Eppendorf, Westbury, NY). The following equation was used to determine the number of molecules of amplicon per microliter.

Length of temp in bp x 660 da/bp = daltons

$1x10^{6}$ da molecules = 1µg/pmole

1mole has $6.02x10^{23}$ molecules = $10^{12}$ pmoles

1pmole = $6.02x10^{11}$ molecules

Example:

Amplicon is 102 bp and concentration is 133.92 μg/ml (0.13392 ng/μl)

102bp x 660 da/bp = 67,320 da

0.067320 ug/pmole

$0.067320/6.02x10^{11} = 0.13392/x$

$x = 1.198x10^{12}$ molecules per1μl

A series of 1/10 dilutions was completed using the purified PCR product and nuclease-free $dH_2O$ to create the template for the standard curve of molecule number vs. $C_T$.

**Calculation of Fungal Burden per Lens**

Fungal burden per lens is expressed as conidial equivalents per lens (CE / lens). To determine the CE / lens, CE determined from the qPCR assay was divided by 2 (number of microlitres of template DNA used in the qPCR reaction) to determine the CE/μl. The CE/μl was then multiplied by the volume of buffer used in DNA resuspenion to determine the CE/lens.

**Construction of a Disruption Vector**

A 1.2 kb fragment of *fmk1* was amplified from genomic DNA isolated from AFR4 by amplification with primers OLIFMK1 and OLIFMK2 (14). The amplification included an initial denaturation of 94°C for 5 minutes, followed by 35 cycles of 94°C 35 seconds, 58°C 35 seconds, 72°C 90 seconds and a final extension of 72°C for 10 minutes. Amplicons were cloned into pGEM T Easy (Promega, Madison, WI) and transformed into *E. coli* JM109 competent cells following the manufacturers' recommendations.

Genomic DNA was isolated from ATCC strain MYA-1774 and a phleomycin resistance cassette was amplified with primers GPD2K and TRP2K (Mattern et al., 1988). A 2.8 kb amplicon was gel purified, cloned into pGEM T Easy (Promega, Madison, WI) and transformed into *E. coli* JM109 competent cells by heat shock transformation. Transformants were selected based on blue-white screening and selected clones were sequenced at the Georgia State core facility to ensure the proper insert.

The vector containing the *fmk1* gene encoding MAP kinase was digested with Kpn I and dephosphorylated with calf intestinal alkaline phosphotase to prevent religation of the vector. The phleomycin resistance cassette was released by digestion with KpnI and the vector and insert were ligated using Fast-Link DNA Ligase (Epicentre, Madison, WI) following manufacturers' recommended protocols. The ligation product was transformed into *E. coli* JM109 by heat shock transformation. Colonies were screened by PCR using the OLIFMK1/OLIFMK2 primer set. Clones selected yielded an ~ 4kb amplicon. This amplicon was PCR purified using a Qiagen PCR Purification kit and used as "transforming" DNA for fungal transformation.

**Protoplast Formation**

Conidia of AFR4 were harvested from 5 day old PDA plates as described by Crow et al. Approximately $10^9$ conidia were inoculated into 100 ml of PDB and shaken at room temperature for 10-14 hours to allow for >90% germination. The germinated conidia were washed twice with 2X OB (1.4 M $MgSO_4$, 50mM sodium citrate [pH 5.8]). Conidia were then digested with 10 ml OB-10% Glucanex (Sigma, St. Louis, MO ) at room temperature until greater than 90% protoplasts were visible, usually within 4-8 hours (15). Protoplasts were filtered through sterile cotton plugs in pasteur pipettes and centrifuged at 1500 x g, 30 minutes, $4^oC$. The protoplasts

were aspirated from the top of the suspension and washed twice with TB (1.0 M sorbitol, 50mM NaCl, 10mM Tris chloride[pH 7.4]). They were then resuspended at $10^8$/ml in TB-6% PEG 4000-1% dimethly sulfoxide and stored at –80$^o$C.

**Fungal Transformation**

Fungal transformation was done with modification to the protocol of Malardier et al (32). Briefly, $10^7$ protoplasts were incubated on ice for 20 minutes. To the protoplasts, 5 μg transforming DNA was added and the reaction was incubated for 20 minutes at room temperature. To the reaction, 160 μl 60% PEG 4000/10mM Mops were added and the reaction was incubated 15 minutes at room temperature. One ml of MSC was added and the protoplasts were pelleted at 12000 x g for 5 minutes at 4$^o$C. The supernatant was discarded and the protoplasts were resuspended in 200 μl MSC. Transformed protoplasts were plated onto minimal media, adjusted to pH 8, and supplemented with 50-100 μg / ml phleomycin. Monoconidial suspensions were isolated and gene replacement was verified by spore PCR with primers OLIFMK1 and OLIFMK2.

**Construction of Fungal Growth Chambers**

Fungal growth chambers were constructed using Fisher*finest* 35x50 mm premium cover glass (Fisher, Pittsburgh, PA) spaced with 5 Corning cover glass No. 1, 24x60 mm, 0.13mm thickness (Corning, Corning, NY) and commercially available blue RTV silicone sealant. For construction of the chamber, 2 cover glass where placed together with five smaller glass 0.13 mm thick sandwiched in between. A thin layer of RTV was placed along the 3 edges. The RTV was spread with a syringe tip to ensure a complete seal and dried overnight. After curing, the

chambers were place in a beaker and autoclaved. The sterile chambers were filled with media as described in each assay and physiology determined. Figure 3 depicts a fungal growth chamber poured with nutrient agar and 1.5% technical agar containing bromo-cresol purple. The yellow layer indicated the technical agar while the purple indicated the interface between nutrient and technical agar.

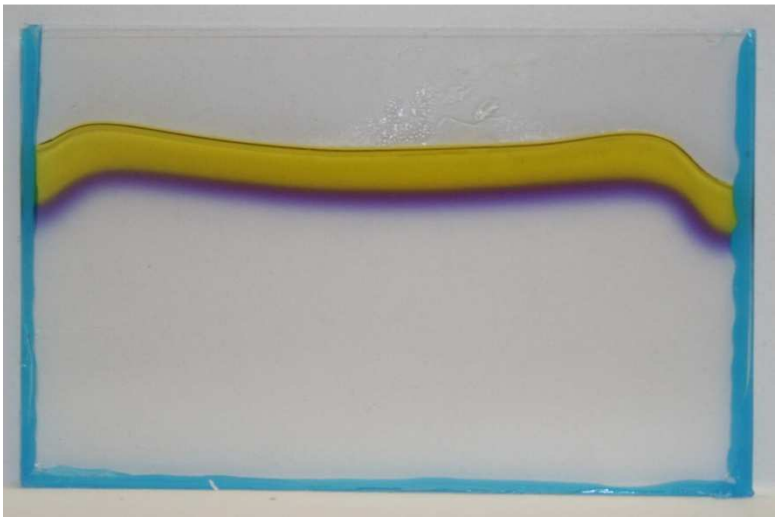

Figure 3. Fungal growth chamber with yellow technical nutrient layer, purple interface and clear Czapek Dox nutrient layer. The chamber is 35mm x 50 mm x 0.65 mm and sealed with blue all purpose gasket maker.

**Germ Tube Emergence**

To determine the polarity of germ tube emergence in a growth chamber, chambers were filled with potato dextrose agar within 1 inch of the surface. The media was allowed to solidify and the chambers were inoculated with 20-30 µl ~$10^6$spores/ml AFR4 or AFR4$\Delta$*fmk1* conidial suspension. Chambers were incubated at room temperature, vertically, and germination was monitored hourly by wide field microscopy to determine polarity of germ tube emergence.

**Comparative Growth of AFR4Δ*fmk1***

A growth curve was completed using wet weight measurements for comparison of growth rates of AFR4 and AFR4Δ*fmk1*. Tubes containing 5 ml of Czapek Dox broth were inoculated with $10^4$ spores of AFR4 or AFR4Δ*fmk1* and incubated at room temperature with shaking at 40 rpm. Duplicate weights were taken at 12, 24, 45, and 96 hours by vacuum filtration onto 0.45 μm filter.

**Chemotropism of ΔMAPK**

The role of MAP kinase signaling pathways in chemotropism was investigated using the fungal growth chamber. To determine if *fmk1* plays a role in chemotropism, the fungal growth chamber was filled to mimic an eye covered by a hydrogel contact lens. To create this model, the fungal growth chamber was poured within ½ inch of the top with a nutrient agar. This layer was cooled and then covered with ~ ¼ inch of technical agar. After the agar had solidified, the chambers were inoculated with 20-30 μl of ~$10^6$ spores/ml of wild-type or AFR4Δ*fmk1* and incubated at room temperature. Penetration was monitored by microscopy over a 48 hour period, with differences in penetration rate and spore germination graded.

**Chemotropism with a Nutrient Gradient**

A nutrient gradient was created by placing a ½ inch filter disk saturated with Czapek Dox Broth (CDB) onto one edge of a 1.5% agar plate containing bromo-cresol purple. A 10 μl drop with $10^2$, $10^3$, or $10^4$ conidia of AFR4 or AFR4Δ*fmk1* was spotted near the opposite wall of the plate. Plates were incubated at room temperature for 72 hours. Growth was measured as was the

radius of growth towards the nutrient disk. These values were used to calculate a percent growth towards nutrient to determine the role of fmk1 in chemotropism.

**Spore Adherence to Hexadecane**

Spore surface hydrophobicity was compared using a modification of the BATH (Bacterial Adherence To Hexadecane) assay. In the modified assay, 1 ml of 0.7-1.0 $A_{440}$ spore suspension of AFR4 or AFR4∆*fmk1*, was transferred to a 2 ml microfuge tube containing 0.5 ml hexadecane. The sample was vortexed for 2 minutes at high speed and then allowed to separate for 15 minutes at room temperature. The aqueous phase was then removed to a cuvette and $A_{440}$ measured. To calculate percent hydrophobicity the following formula was used: $100(A_0-A_f)/ A_0$ where $A_0$ is the initial absorbance and $A_f$ is the final absorbance.

**Preparation of Porcine Eyes**

In order to ascertain the role of MAP kinase in the penetration of contact lenses by *F. solani*, porcine eyes were obtained from River View Farms (Ranger, GA). The eyes received included surrounding skin and fur. The skin, eyelid and membrane were resected leaving only the globe and optic nerve. The eyes were surface sterilized in 10% bleach and then rinsed three times in sterile saline. Eyes were placed in sterile glass jars filled with saline and stored at $4^oC$.

**Mitogen Role in Penetration of Contact Lenses**

The role of an animal mitogen in penetration of contact lenses was determined using porcine eyes. The hydrogel lens was placed over the cornea of a porcine eye. The exposed surface of the lens was then exposed to saline, $10^4$ conidia of AFR4, or $10^4$ conidia of

AFR4Δ*fmk1*. The eye with lens was place into 30 mls of sterile saline and incubated at room temperature 24 hours. The lenses were removed from the eyes, stained with 50mM Syto59 (Invitorgen, Carlbad, CA.), 120 minutes and imaged using a Texas Red filter (Ab 622, Em 645 μm).

**Role of Map Kinase in Penetration of Contact Lenses**

Commercially available silicone hydrogel lenses were removed from storage solution and rinsed with then soaked in phosphate buffered saline (PBS) for 2 hours. The lenses were placed into scintillation vials containing 3 mls of PBS with $10^5$ conidia AFR4 or AFR4Δ*fmk1* and incubated for 5 days at room temperature with orbital shaking at 40 rpm. The lenses were removed from solution and prepared for Scanning Electron Microscopy (SEM).

**Scanning Electron Microscopy**

Contact lenses to be prepared for scanning electron microscopy (SEM) were rinsed in phosphate buffered saline (PBS) three times. PBS was removed from the scintillation vials and samples were fixed with gluteraldehyde, postfixed with with 1% $OsO_4$, and subsequently dehydrated with increasing concentrations of acetonitrile. Lenses were then dried at $40^0$C and fixed to a metal stub. The lenses were sputter coated with AuPd and imaged.

**Role of Map Kinase in Tissue Penetration**

Fungal growth was monitored after microinjection of conidia into the cornea of porcine eyes to determine the role of MAP kinase in tissue penetration. Porcine eyes were removed from saline and 50 μl of either saline or a $10^5$ conidial suspension of AFR4 or AFR4Δ*fmk1* was

injected ~1/4 inch beneath the surface. Each eye was placed in a glass jar filled with saline and incubated at room temperature. At 24 hour intervals the degree of hyphal invasion of the cornea was recorded and photographed. The eyes were also graded for firmness and photographed to mark deterioration. After 72 hours, samples were taken from the center of the globe at 10 mm intervals measuring back from the cornea. DNA was extracted using a Qiagen DNeasy Tissue kit and PCR was performed using primers AFRBTF and AFRBTR to determine the extent of fungal penetration through the eye.

## III. RESULTS

### Identification of Proteins Associated with Contact Lens Penetration by *F. oxysporum* AFR9

In SDS-PAGE, to identify novel proteins associated with contact lens penetration by *F. oxysporum* AFR9, several bands were identified as being upregulated in lens-associated samples during comparative protein analysis of planktonic vs. lens-associated *F. oxysporum* AFR9. The four bands are illustrated in Figure 4. The proteins were unable to be identified by Maldi TOF-TOF analysis.

### Determination of Fungal Burden on Contact Lenses

Traditional methods for detection of fungal burden require microscopic or plate counts and can be time consuming and inaccurate, often require the use of high density inocula unlike conditions seen in the real world. To reduce the inaccuracies seen in traditional methods, a method for determination of fungal burden on contact lenses was developed using qPCR. With this method small inoculums can be utilized and low numbers of lens associated conidia can be detected. Detection was possible with as few as 5 conidia, Figure 5. The qPCR assay developed was used to determine the role of FMK1 in AFR4 association with contact lenses. For this assay, commercially available hydrogel contact lenses were exposed to $10^4$ conidia of AFR4 or AFR4$\triangle$*fmk1* in 3 ml saline for 24 hours. DNA was then extracted and fungal burden per lens determined. On control lenses no detection occurred while on AFR4 exposed lenses an average of 431 conidia were detected. Lenses exposed to conidia of AFR4$\triangle$*fmk1* averaged 63 associated conidia per lens, Figure 6, a significant decrease from wild-type associated conidia in triplicate samples.

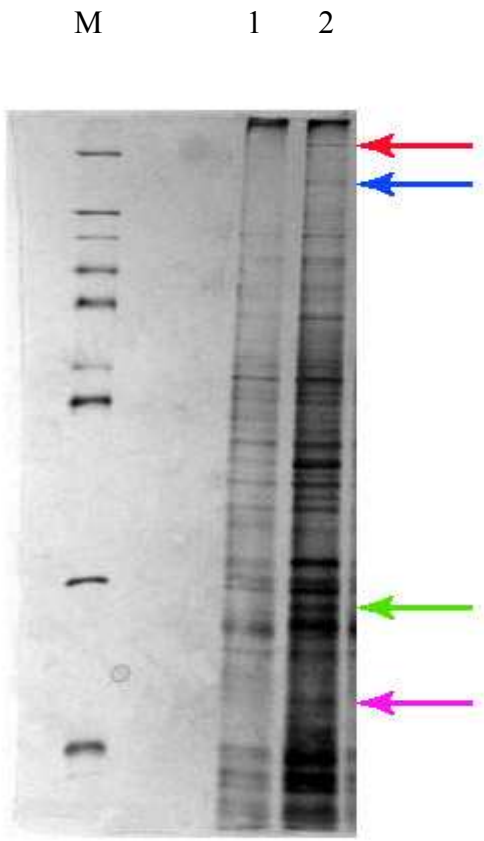


Figure 4: SDS-PAGE silver stained gel depicting proteins upregulated in lens-associated samples during comparative protein analysis of planktonic vs. lens-associated *F. oxysporum* AFR9. Lane 1 represents proteins isolated from AFR9 and lane 2 represents proteins isolated from lens-associated AFR9. The arrows indicated proteins identified in attached samples. Approximated sizes are: red 205,000 kDa protein, blue arrow 105,000 kDa protein, green arrow 30,000 kDa protein, and purple arrow a 25,000 kDa protein.

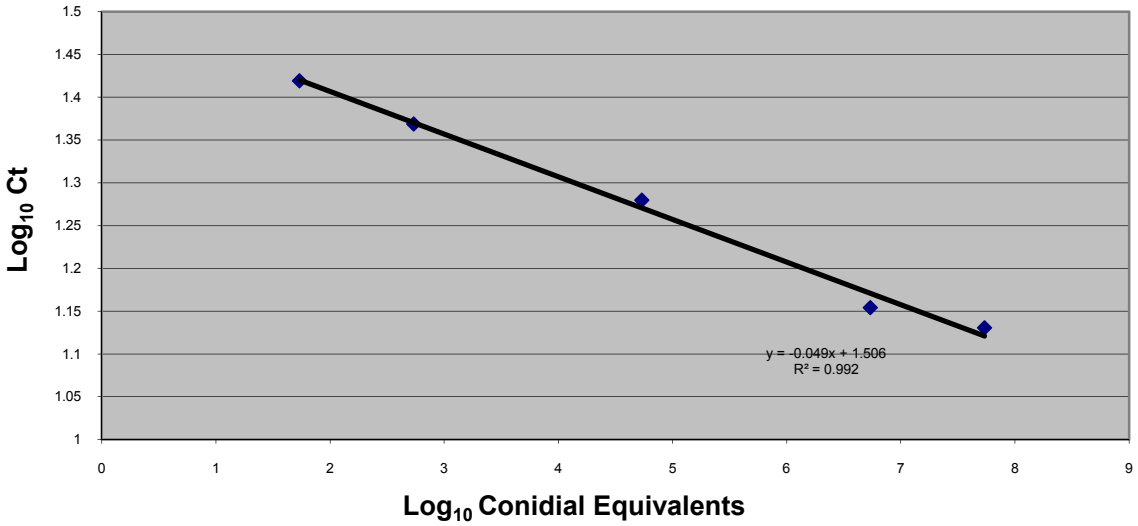


Figure 5: Determination of conidial equivalent detection range. Conidial equivalents were detected from 48,000 to 4.8 CE.

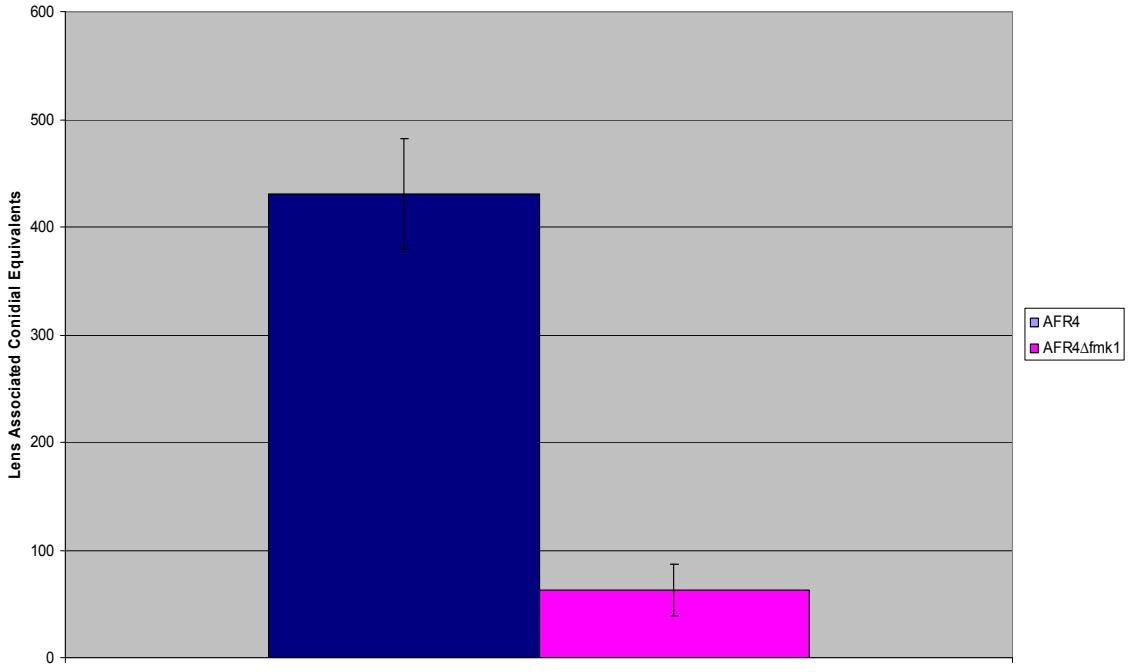


Figure 6: Comparison of AFR4 and AFR4Δ*fmk1* conidia associated with commercially available hydrogel contact lenses. Values represent triplicate samples.

**Construction of AFR4Δ*fmk1***

AFR4Δ*fmk1* was created using one-step gene replacement. Construction of a gene replacement vector was achieved by amplifying the 1.2 kb *fmk1* gene from *F. solani* AFR4 with subsequent cloning into pGEM-T Easy to create pGEM::*fmk1*. A phleomycin resistant cassette was amplified from *A. nidulans* MYA-1774 and primer set OliFMK1/2 (24). The cassette was cloned into the KpnI site located downstream of the threonine and tyrosine residues of FMK1. The disrupted *fmk1* gene was PCR amplified and used to transform *F. solani* AFR4 as in Figure 7. Transformants were selected on CDA supplemented with 100 µg/ml phleomycin. Gene replacement was verified by PCR with primers OliFMK1 and OliFMK2. Amplicons of wild-type AFR4 *fmk1* were 1.2kb while positive transformants yielded a 3.8kb band as seen in Figure 8.

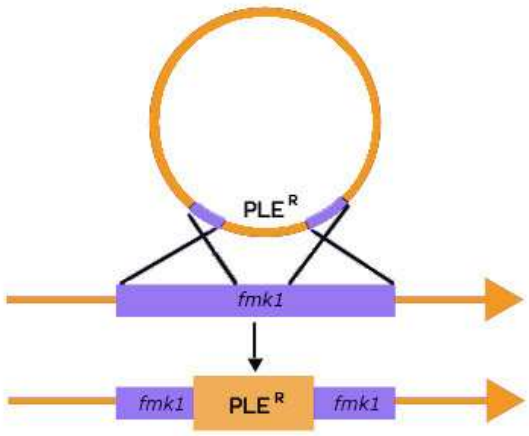


Figure 7: One step gene replacement strategy used to create AFR4Δ*fmk1*. The *fmk1* gene was disrupted by insertion of a phleomycin resistance cassette, cloned behind a *gpdA* promoter, amplified from *Aspergillus nidulans*. The product was PCR amplified for transformation into *F. solani* AFR4; homologus recombination resulted in AFR4Δ*fmk1*.

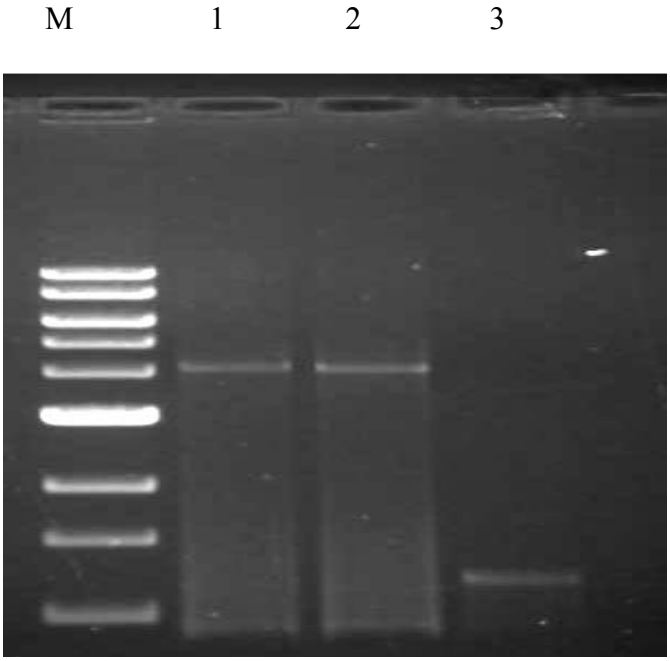


Figure 8: 0.8% Agarose gel with amplification using OliFMK1/2. Lane 1: AFR4△*fmk1*, Lane 2: gene replacement plasmid DNA, and Lane 3: AFR4 wild-type, M: 1kb molecular weight marker.

**Germ Tube Emergence is Not Dependent on FMK1**

Upon germination of *F. solani* a germ tube emerges from the conidia. The germ tubes differentiate to hyphae in latter phases of development. Germ tube emergence is often relegated to conidial poles and regulated by environmental conditions (46). The potential role of MAP kinase in germ tube emergence was determined using fungal growth chambers. The chambers were filled within ¼ inch of the top with Czapek-Dox agar and inoculated with AFR4 or AFR4△*fmk1* conidia. The chambers were monitored hourly for germ tube emergence. After approximately 6 hours of incubation greater than 80% of the conidia had germinated. Germ tubes appeared to emerge from poles of the conidia without chemotropic influence. Figure 9 depicts germ tube emergence from AFR4 and AFR4△*fmk1*. The germ tubes emerging from AFR4 appear to emerge randomly, but can be seen immediately turning down towards the

nutrient source while germ tubes emerging from AFR4△*fmk1* appear to continue growth without chemotropic influence. Germ tubes emergence from both poles was frequently observed in AFR4△*fmk1* as in Figure 9 (B).

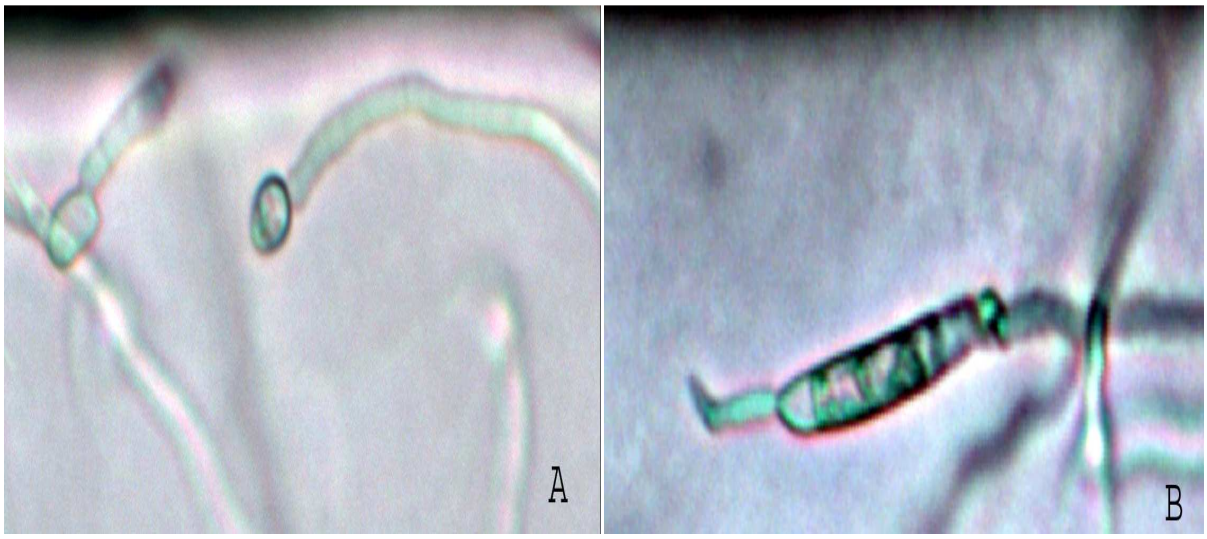


Figure 9: Germ tube emergence was determined using fungal growth chambers filled with Czapek-Dox agar. AFR4 (A) can be seen emerging from microconidial poles while in AFR4△*fmk1* (B) germ tubes are emerging from macroconidial poles. AFR4 germ tubes turn immediately towards nutrient once differentiated to hypae while AFR4△*fmk1* appear to continue in random directions.

**Growth Rate is Not Affected by FMK1**

Growth curves were completed using wet weight measurements from both AFR4 and AFR4△*fmk1*, with samples were taken at 12, 24, 45, and 96 hours post inoculation, illustrated in Figure 10. The rate of growth was equivalent for both the wild-type and mutant strain. Figure 11 depicts equivalent growth over time for AFR4 and AFR4△*fmk1* with a slight lag in growth apparent in the mutant strain from inoculation to twenty hours.

**Chemotropism is Reliant on FMK1**

The role of FMK1 in chemotropism was determined using two different assays. The first utilized fungal growth chambers to model the eye covered by a contact lens. To mimic the eye/lens system, the fungal growth chamber was filled ¾ of the way with Czapek-Dox agar, and then topped with ¼ inch of 1.5% technical agar. The nutrient mimics the eye and the technical agar serves as the lens. The chambers were inoculated with AFR4 or ARF4Δ*fmk1* and incubated 24 hours. At 24 hours, penetration through the technical agar was imaged to determine the role of FMK1. AFR4 spores were able to germinate and germinules immediately turned toward the nutrient while

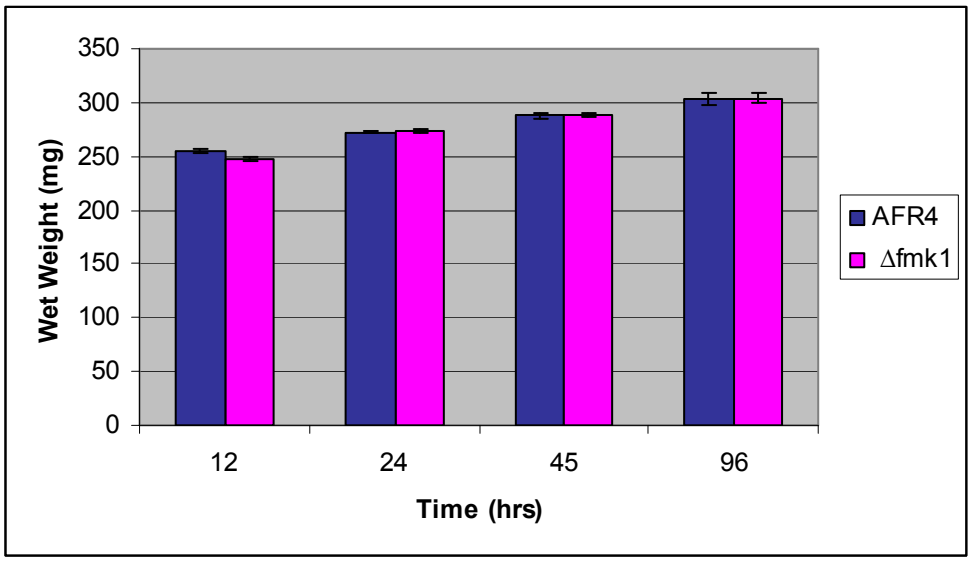


Figure 10: Comparison of weight weights after 12, 24, 45 and 96 hours of growth in Czapek-Dox broth.

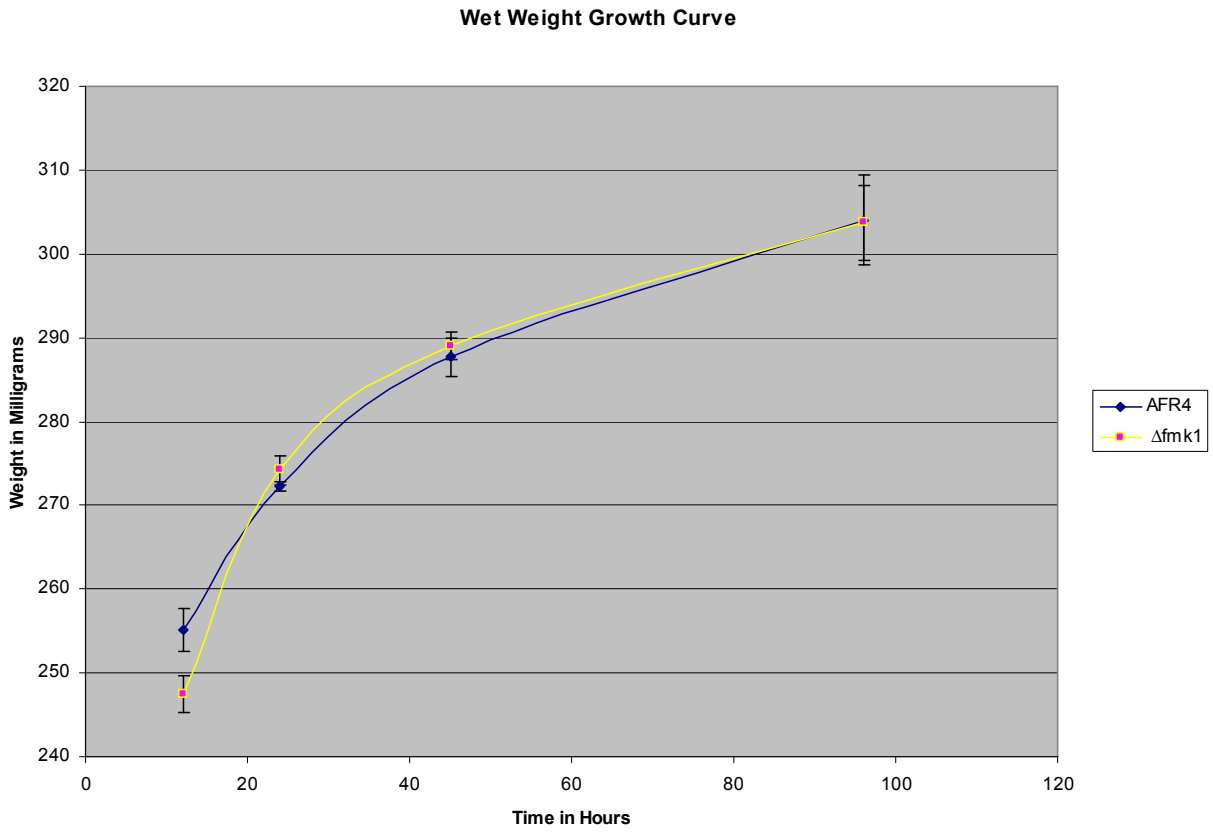


Figure 11: Wet weight growth curve showing equivalent growth rates for AFR4 (blue) and AFR4Δ*fmk1* (yellow).

AFR4Δ*fmk1* displayed a markedly different pattern. The mutant strain was able to germinate but growth towards the nutrient layer was not directed, Figure 12. The hyphal growth of AFR4Δ*fmk1* penetrated through the technical agar layer aimlessly, and less hyphal growth was noted.

A second assay was performed to determine the role of FMK1 in chemotropic behavior of *F. solani* AFR4 in the presence of a nutrient gradient. In this assay, a filter disk saturated with Czapek-Dox broth was placed at one edge of a 0.5% agar plate containing bromo-cresol purple. Across the plate from the disk, 10 µl spots of $10^2$, $10^3$, or $10^4$ conidia of AFR4 or AFR4Δ*fmk1*

were spotted. The number of conidia spotted was varied to determine if quorum sensing affected chemotropic behavior. The nutrient diffused through the agar to create a gradient. After 72 hours, the diameter of growth was measured as well as the radius of growth towards nutrient. These values were used to determine the percent growth towards nutrient, Figure 13. A percent growth towards nutrient of >50% indicated chemotropism. After 72 hours of growth, there was no variation in percent growth towards nutrient based on density of conidia present in inoculum in either strain. An obvious difference was visible in percent growth towards nutrient in AFR4 vs. AFR4Δ*fmk1*, Figure 14. In AFR4, germination and growth initially occurs in all directions but after 24 hours a greater percentage of growth is directed towards the nutrient source. In AFR4Δ*fmk1*, growth appears to be stunted by inability to sense nutrient. Growth and germination are intitially identical to that of AFR4, but after 72 hours, hyphal growth has not progressed in the direction of the nutrient.

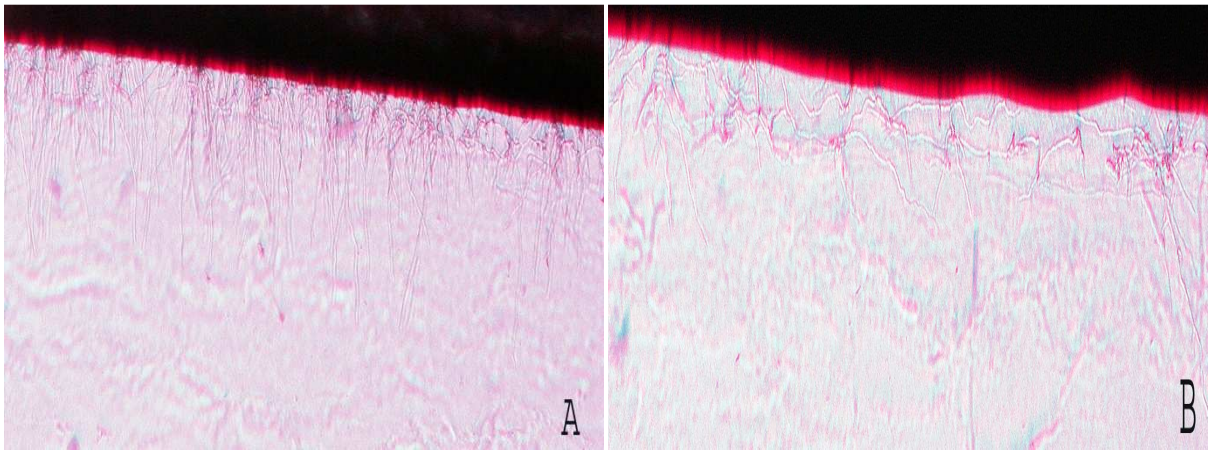


Figure 12: Penetration through and eye/lens model developed using fungal growth chambers. The chamber contains ¾ CDA and ¼ inch 1.5% technical agar. Conidia of AFR4 are able to germinate and germinules immediately turn towards the nutrient source. AFR4Δ*fmk1* are also able to germinate, but are unable to sense the nutrient source and travel through the technical agar aimlessly.

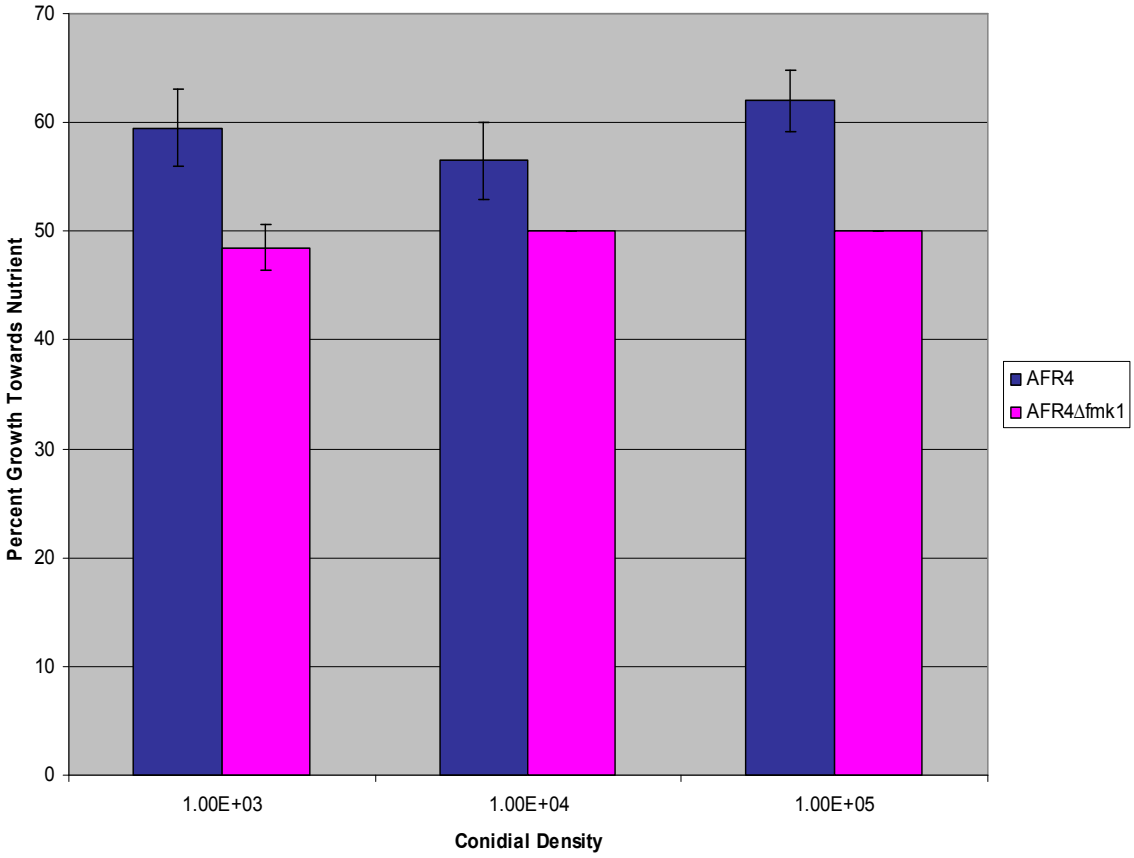


Figure 13: Comparison of AFR4 and AFR4△*fmk1* chemotropism. Percent growth towards a nutrient source was measured by determining the diameter of overall growth and the radius of growth towards nutrient. AFR4, with a percent growth towards nutrient of >50%, demonstrates chemotropism while AFR4△*fmk1*, with a percent growth towards nutrient of ≤ 50% demonstrates no chemotropic ability. Quorum sensing does not appear to influence chemotropism as conidial density is insignificant.

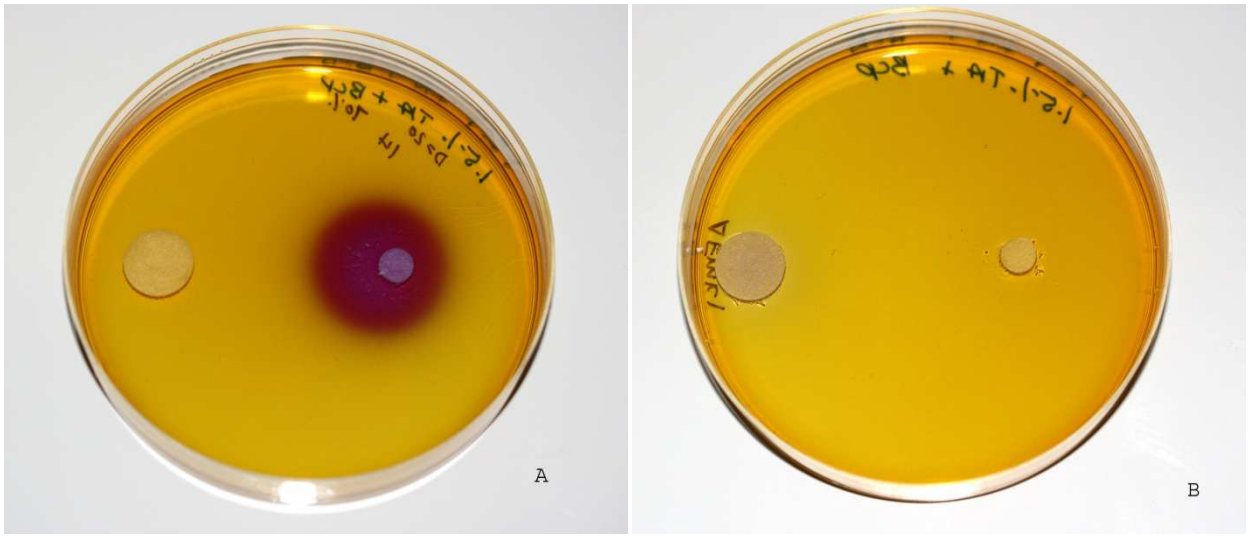


Figure 14: Plate assay for determination of the role of FMK1 in chemotropism in the presence of a nutrient gradient. AFR4 (A) displays chemotropism towards the nutrient source after 72 hours while AFR4Δ*fmk1* (B) is only able to germinate and grow immediately adjacent to the site of inoculation.

**Disruption of *fmk1* Alters AFR4 Morphology**

In *F. solani* AFR4 disruption of the *fmk1* gene with a phleomycin resistance cassette leads to alteration in morphological characteristics. Wild-type AFR4 when plated onto agar presents diffuse growth which quickly covers the entire Petri plate. Disruption in *fmk1*, results in less diffuse growth on agar yielding a colony-like appearance as shown in Figure 15. At 7 days, growth by AFR4Δ*fmk1* is mostly fluffy white but begins to pigment between 7-10 days. Agar is chocolate colored with dark growth after 14 days while AFR4 remains fluffy and white.

Disruption of MAP kinase produces not only changes in morphology but also changes in conidiation. *F. solani* AFR4 produces both microconidia and macroconidia when grown on CDA with microconidiation occurring preferentially, Figure 16A. FMK1 affects conidiation patterns in *F. solani*; AFR4Δ*fmk1* preferentially produces macroconidia over microconidia as seen in Figure 16B. Disruption of *fmk1* also affects germination of microconidia in non-nutrient

environments. Conidia from both mutant and wild-type strains were incubated in PBS for 4 days with a commercially available hydrogel contact lens. Microconida germination is visible in AFR4 while only macroconidia germination is visible in AFR4△*fmk1*, Figure 17. During growth on Czapek-Dox agar microconidia of AFR4△*fmk1* are able to germinate and germ tubes later differentiate to hyphae as seen in *F. solani* AFR4.

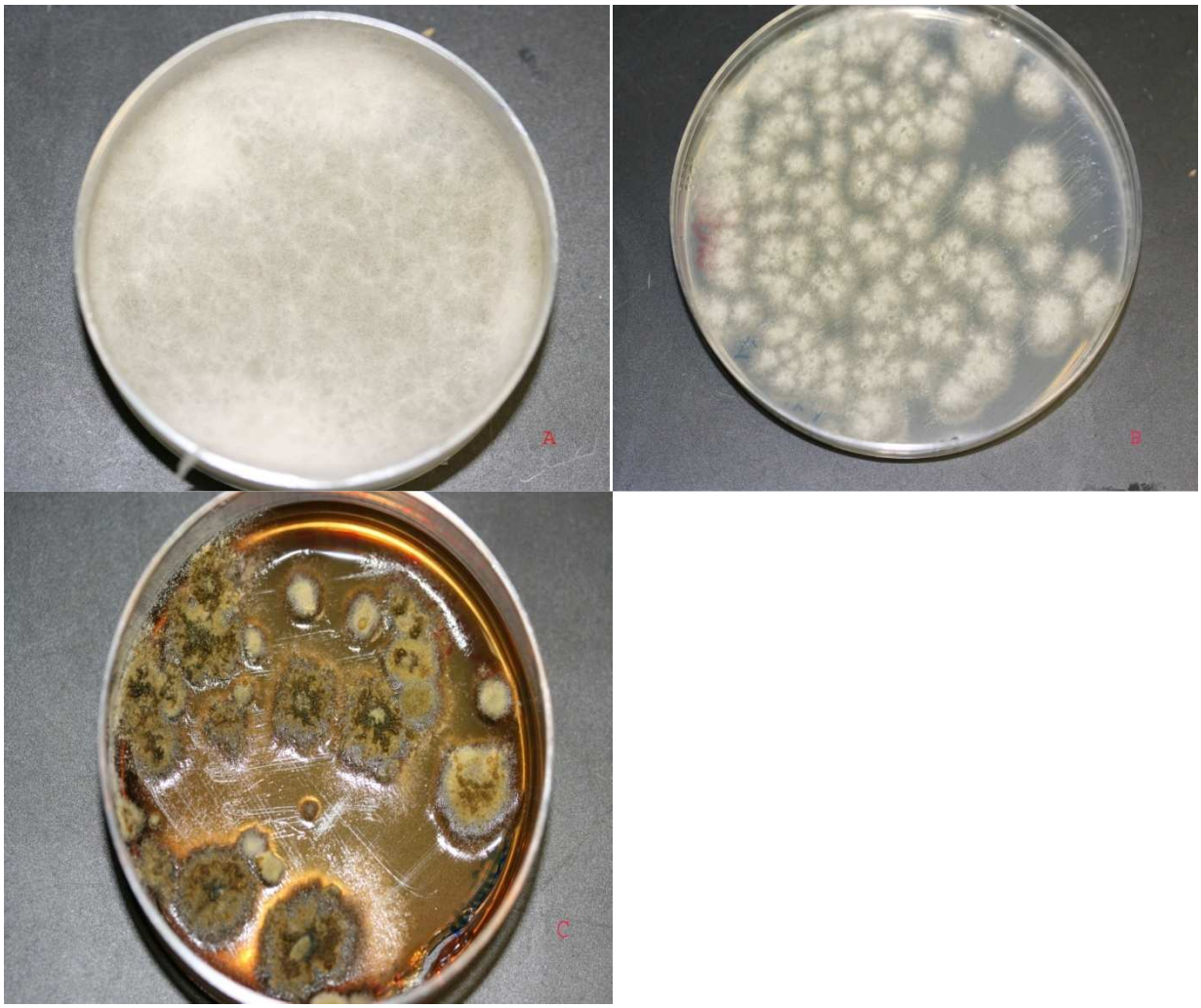


Figure 15: Fluffy white growth can be seen covering Czapek-Dox agar after 7days of growth by AFR4 (A). After 7 days of growth on Czapek-Dox agar AFR4△*fmk1* produces fluffy white colony-like growths (B) which begins to turn dark nearing 10 days growth and become pigmented near 14 days (C).

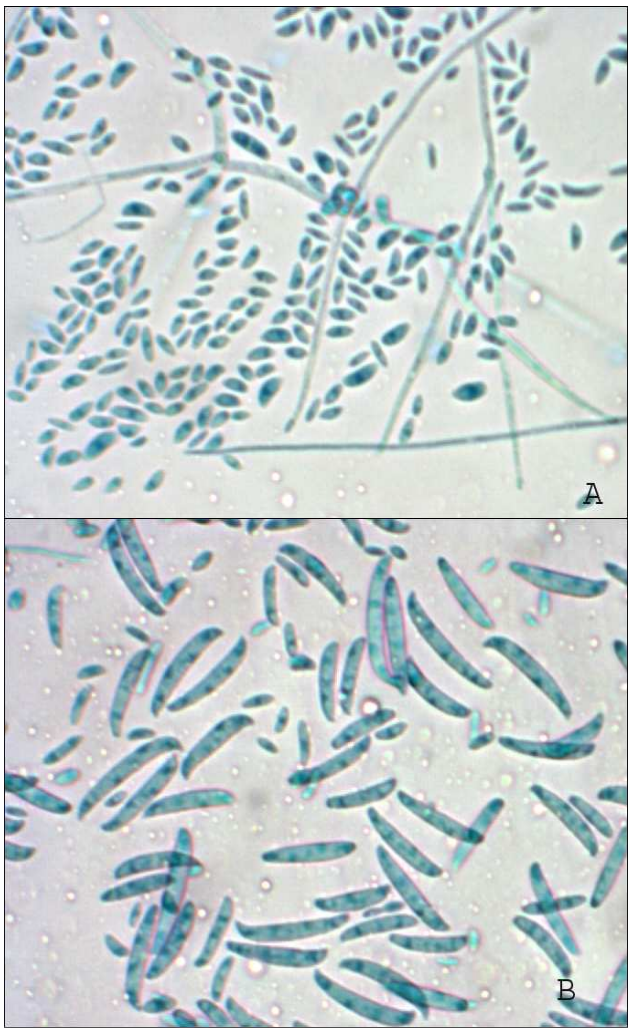


Figure 16: Difference in conidiation patterns can be attributed to FMK1. *F. solani* AFR4 grown on CDA favors the production of microconida (A) while the majority of conidia produced by AFR4∆*fmk1* when subjected to identical growth conditions are macroconidia.

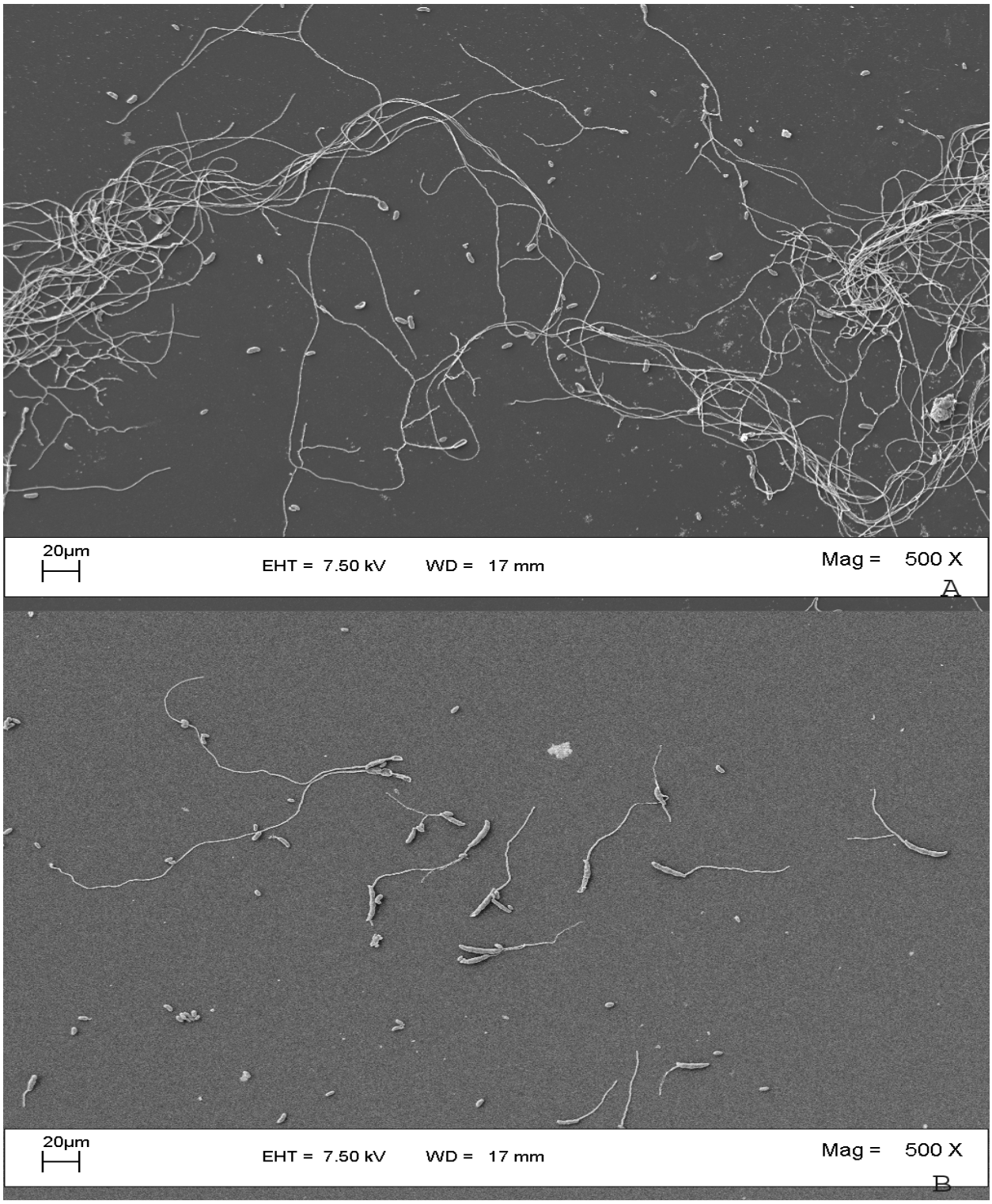


Figure 17: Conidia germination is affected by disruption of *fmk1* in non-nutrient conditions. AFR4 microconidia germinate regularly in PBS (A) while only macroconidia of AFR4∆*fmk1* are able to germinate (B).

**Deletion of MAP Kinase Affects Spore Hydrophobicity**

Commercially available hydrogel and silicone hydrogel lenses are designed to increase surface hydrophilicity. With differences in manufacturing come differences in lens surface hydrophilicity. Spore surface hydrophobicity was determined by adherence to hexadecane in two strains of *F. solani*, AFR4 and AFR4*Δfmk1*. AFR4 percent surface hydrophobicity was determined to be 22% while AFR4△*fmk1* spore surface percent hydrophobicity was 41%. The disruption of *fmk1* increased spore surface hydrophobicity nearly 19% in AFR4*Δfmk1* when compared to wild type AFR4, Figure 18.

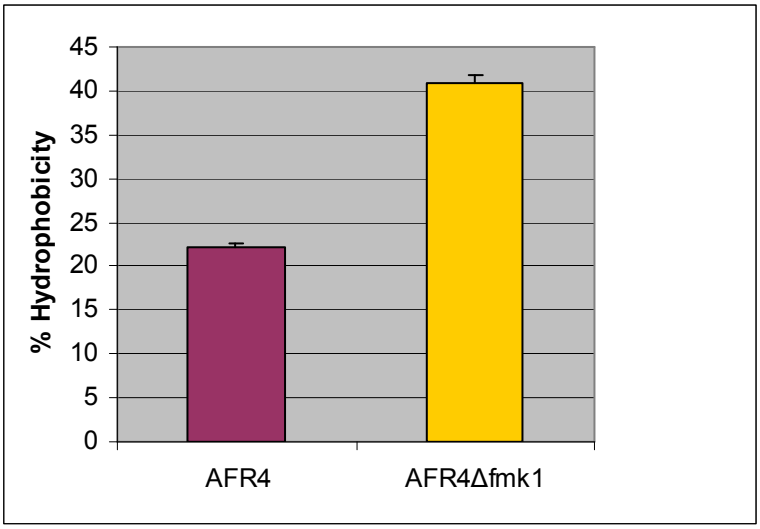


Figure 18: Comparison of spore surface hydrophobicity for AFR4 and AFR4△*fmk1*. AFR4 shows a marked decrease in percent spore hydrophobicity compared to AFR4△*fmk1*. Error bars indicate standard deviation in triplicate samples.

**FMK1 is Responsible for Invasive Growth**

In order to determine the role of FMK1 in invasive growth in tissue, porcine eyes were injected with conidia from AFR4 or AFR4△*fmk1* and incubated for 72 hours with examination

at 24 hour intervals. At 24 hours post-injection, AFR4 injected eyes exhibited diffuse hyphal growth within the cornea with a left lateral spread evident when compared with eyes injected with AFR4△*fmk1*. The AFR4△*fmk1* injected eyes also displayed hyphal growth within the cornea at 24 hours post-injection but growth was highly localized to the site of injection. Saline injected control samples demonstrated no clouding of the cornea at 24 hours post-injection. The AFR4 injected eyes yielded slightly to pressure with sterile forceps while the saline control and AFR4△*fmk1* injected eyes remained firm. Figure 19 depicts the difference in hyphal spread through the cornea at 24 hours post-injection in wild-type vs. mutant strains of *F. solani* AFR4.

At 48 hours post-injection, both saline injected controls and AFR4△*fmk1* injected eyes displayed some "give" when the globes were manipulated. Eyes injected with AFR4 demonstrated mild global flaccidity under pressure with forceps. All injected samples are still round with convex corneal tissue. Visible in Figure 20, both the AFR4 injected and AFR4△*fmk1* injected corneas have clouded completely with hyphal growth while saline injected control tissue remained relatively clear.

Eyes were examined prior to dissection at 72 hours. At this point there was a marked difference in control vs. mutant samples and mutant vs. wild-type samples. At 72 hours post-injection, the control samples were still relatively firm and the corneal tissue convex while the globes injected with AFR4△*fmk1* appeared medially flaccid, the corneas remained convex. In comparison with the AFR4△*fmk1* injected eyes, those injected with wild-type AFR4 displayed total flaccidity with concaved corneal tissue as evident in Figure 21. Corneal tissue of saline injected samples had clouded, but did not display hyphal growth while both wild-type and mutant injected cornea were consumed by hyphae.

At 72 hours post-injection, the porcine eyes were dissected and the lens, vitreous humor, and base of the optic nerve were removed as depicted in Figure 22. Total DNA was extracted from the dissected tissues and PCR was performed to detect invasive spread of *F. solani*. Tissue penetration was graded by amplification as shown in Figure 23. *F. solani* AFR4 demonstrated invasive growth throughout the eye with amplicons present from the lens, vitreous humor, and optic nerve. AFR4△*fmk1* did not exhibited invasive growth; amplification occurred only from DNA extracted from tissue of the vitreous humor.

**Contact Lens Penetration is Not Affected by FMK1**

Commercially available silicone hydrogel contact lenses were inoculated with AFR4 or AFR4△*fmk1* in PBS and incubated for 5 days. After 5 days the lenses were prepared for scanning electron microscopy and imaged for fungal penetration. Figure 24 depicts penetration of hydrogel lenses by both the wild-type and mutant strains. The wild-type strain penetrates the lens more frequently than the mutant strain, but potential for penetration is not hindered by the disruption of *fmk1*. In both strains a segment of the hyphal fragment is raised prior to the penetration into the lens. Penetration pegs are similar in appearance in both AFR4 and AFR4△*fmk1*.

MAP kinases respond to extracellular stimuli known as mitogens. To determine if animal mitogens play a role in lens penetration, a commercially available hydrogel lens was placed over a porcine cornea and the extrerior surface of the lens was inoculated. After 24 hours of growth the lens was removed, stained with Syto59, and examined. Conidia were present on both sides of the lens without penetration through the lens. A second set of lenses was left on the porcine

eyes 9 days at which time they were imaged by SEM. The lenses revealed no penetration and very few conidia if any were visibly associated with this lens type.


Figure 19: Porcine eyes inoculated by microinjection of AFR4 conidia, AFR4Δ*fmk1* conidia or saline (control) 24 hours post-injection. A represents control tissue with no clouding of the cornea. B represents corneal tissue injected with AFR4 conidia; diffuse fungal growth is visible within the cornea extending laterally to the sclera. C represents corneal tissue injected with AFRΔ*fmk1* conidia; fungal growth is visible within the cornea but is localized to the injection site. D represents porcine samples upon receipt.

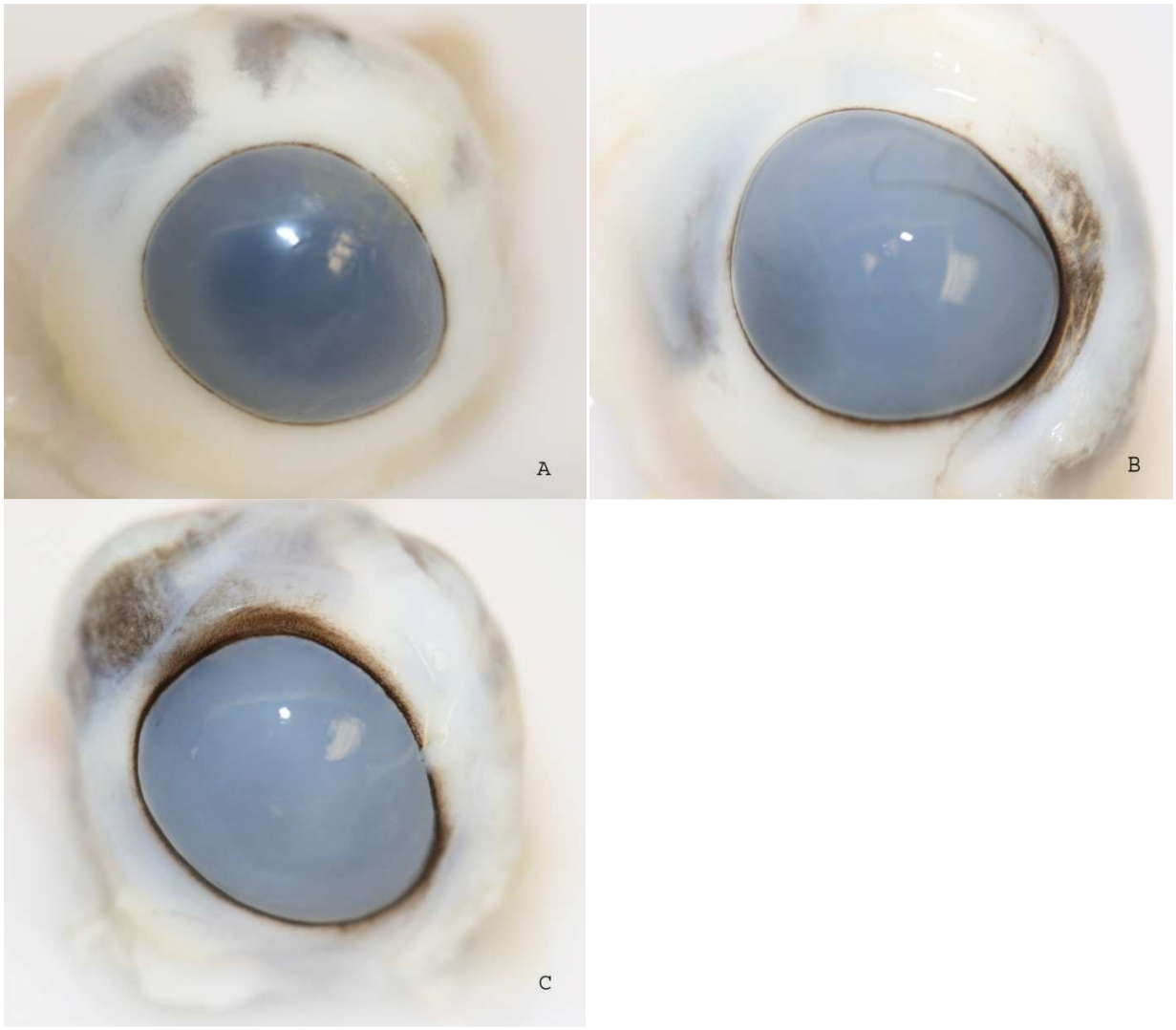


Figure 20: Porcine eyes inoculated by microinjection of AFR4 conidia, AFR4Δ*fmk1* conidia or saline (control) 48 hours post-injection. Saline injected control with relatively clear corneal tissue. AFR4 injected sample (B) shows complete clouding of the cornea due to hyphal invasion as well as marked global flaccidity. AFR4Δ*fmk1* injected sample (C) with complete clouding of the cornea due to hyphal invasion.

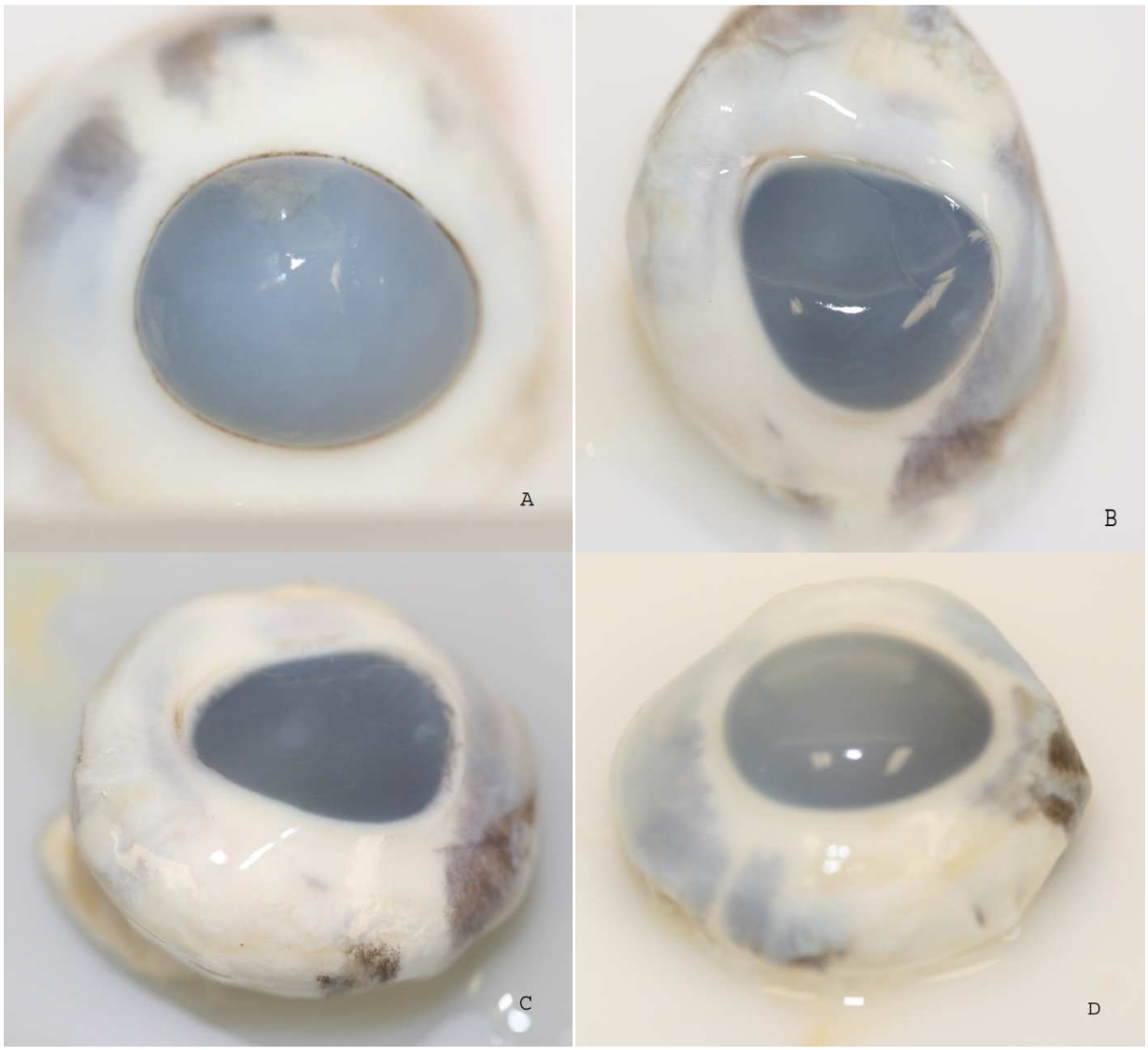


Figure 21: Porcine eyes inoculated by microinjection of AFR4 conidia, AFR4Δ*fmk1* conidia or saline (control) 72 hours post-injection. Saline injected control (A) has clouding of the cornea but still presents convex corneal tissue and a firm globe. AFR4 injected samples (B,C) display clouded corneal tissue as well as global flaccidity. AFR4Δ*fmk1* injected samples retain a convex cornea but display medial sagging of the globe.

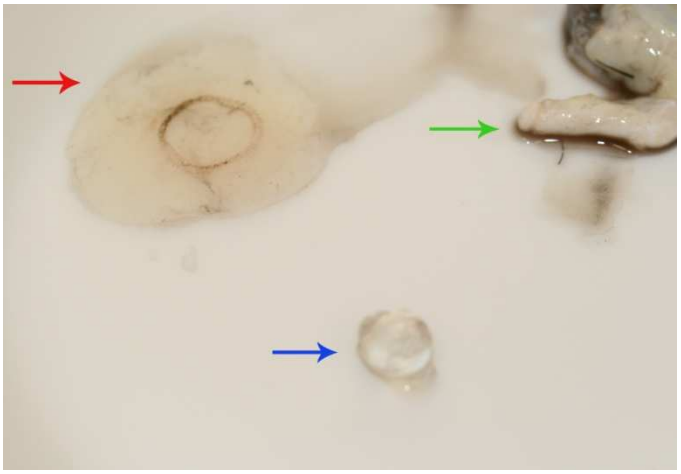

Figure 22: Dissection of injected eyes yielded three tissue samples for DNA extraction. The red arrow marks the vitreous humor, the blue arrow the lens and the green the optic nerve.

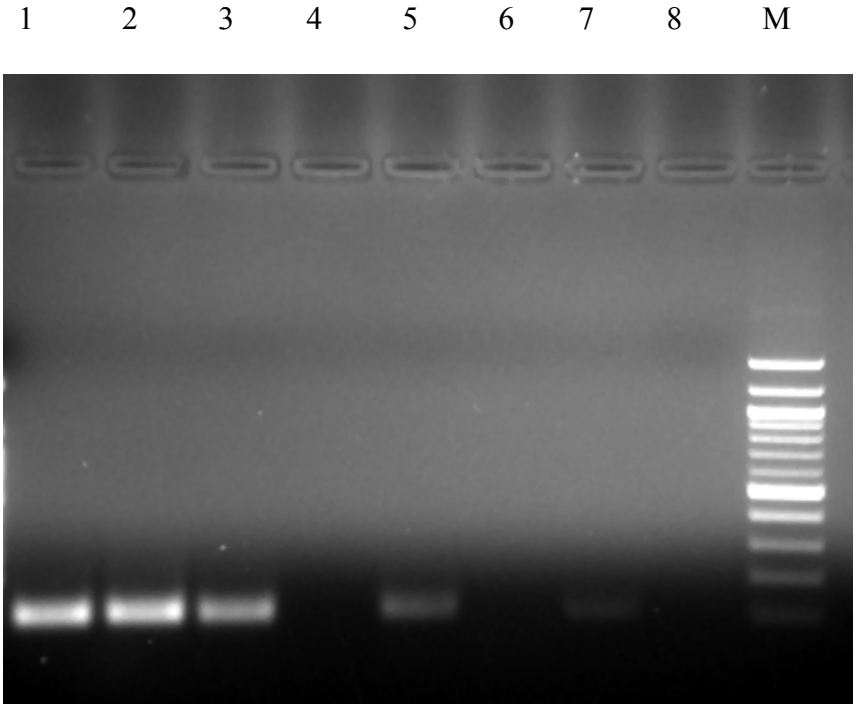


Figure 23: 2% Agarose gel analysis of tissue penetration by AFR4 or AFR4△*fmk1*. Lens of eye inoculated with: *F. solani* AFR4 (lane 1), AFR4△*fmk1* (lane 4), vitreous humor of eye inoculated with: *F.solani* AFR4 (lane 2), *F. solani* AFR4△*mk1* (lane 5), optic nerve of eye inoculated with: *F.solani* AFR4 (lane 3), *F. solani* AFR4△*fmk1* (lane 6). Lane 7 contains a positive control and lane 8 a negative control. 100 bp molecular weight marker (M).

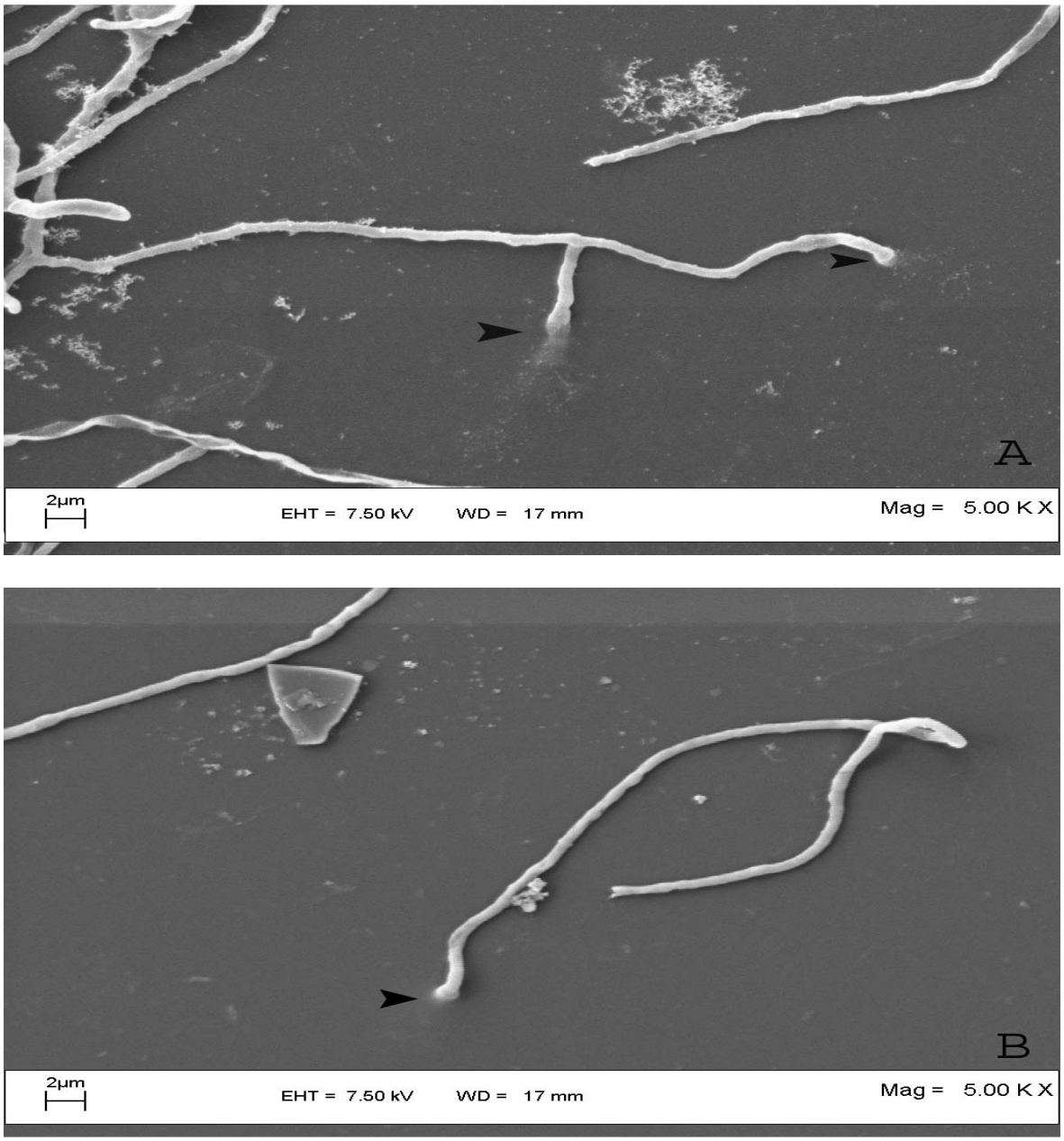


Figure 24: Penetration of a silicone hydrogel contact lenses after 5 days incubation in PBS with conidida of AFR4 or AFR4∆*fmk1*. Black arrows represent penetration into the len by hypae of AFR4 (A) and AFR4∆*fmk1* (B). Penetration occurs in higher frequency by AFR4 as evident in A.

## IV. DISCUSSION

*Fusarium spp.* are soil-born opportunistic pathogens of both plants and animals. Each year they cause significant agricultural damage, decimating crop plants with blight, wilt and canker. The physiologic basis for plant pathogenicity is largely understood, but the molecular basis for pathogenicity-related changes is just being investigated. Recently, DiPietro *et al.*described the role of FMK1, a MAP kinase from *F. oxysporum*, in plant pathogenicity. FMK1 was determined to be necessary for both penetration of the root system and pathogenesis (14).

*Fusarium spp.* have recently garnered attention as ocular pathogens. In 2004, outbreaks of *Fusarium* associated with contact lens wear spurred investigation into the genera with studies being undertaken to identify species which may be pathogenic. Little has been done at this point to understand the mechanisms of pathogenicity in humans. It was the goal of this study to determine the role of the *Fusarium* MAP kinase, FMK1,in the association and penetration of contact lenses.

### FMK1 Affects Morphology

Contrary to previous published results in *F. oxysporum*, where normal growth and conidiation were displayed after disruption of *fmk1*, *F. solani* AFR4$\triangle$*fmk1* exhibited changes in conidiation and morphology (14). Inactivation of *fmk1* lead to small colony-like growth on CDA which would pigment after one week's growth as seen in Figure C while growth in broth cultures was not affected. Along with changes in morphology, changes in conidiation patterns were also noted. Wild-type AFR4 produced copious amounts of microconidia on CDA with the occasional macroconidia present. The opposite pattern is noted for AFR4$\triangle$*fmk1*. The disruption of *fmk1* increases the number of macroconidia produces, Figure 4, and also affects the

germination pattern of these conidia. In the presence of nutrient both maroconida and microconidia are seen germinating while in a non-nutrient environment only macroconidial germination is observed. This may be due to increased phosphate concentrations in the non-nutrient media. Page *et al.* have previously shown phosphate concentration affects macroconidia germination or to the inability of the fungi to sense phosphate concentrations (42).

Surface hydrophobicity greatly influences spore/surface associations. Contact lens surfaces vary greatly depending on construction material and surface treatments. *Acanthamoeba* have been shown to preferentially attach to silicone hydrogel lenses based on the elastomer material used as opposed to surface treatment applications (5). Buffington *et al.* found that penetration of hydrogel lenses is a function of the chemical composition of the lens as well as the ability of fungal species to penetrate polymer (8). Spore surface hydrophobicity is one characteristic influencing fungal association with contact lenses. Inactivation of *fmk1*, increased spore surface hydrophobicity may influence the association of spores with contact lenses. The effect would vary by lens type and surface treatment, but one would expect to see an increase in attachment of wild-type spores as lens surfaces strive to be hydrophilic.

**Determination of Contact Lens Associated Fungal Burden with qPCR**

*Fusarium spp.* has recently garnered much attention as a human pathogen. Until the 21$^{st}$ century most cases of *Fusarium* mycoses were related to trauma, but with the increase in the number of immune compromised individuals as well as increased contact lens wear, *Fusarium spp.* has revealed itself as opportunistic. Being able to detect and quantify fungal samples at very low levels was previously difficult as identification is often based on morphological characteristics. These characteristics are often difficult to identify and the observer may bias identification of fungal species. Quantification has also been tedious and often inaccurate, as it

has been based on dilution plating methods. Plate counts can prove problematic due to the fact that many plates become overgrown before morphological characteristics are well developed and can be used to both identify and quantitate fungal genus and species (39).

In this study, a method was developed to both quickly and accurately quantitate *Fusarium* conidial equivalents. A method employing qPCR facilitated the detection of as few as 4.8 CE. The qPCR method eliminates the need for cultivation of fungal species decreasing the time involved while increasing accuracy and range limits of quantitation. The qPCR method can be used to quantitate CE from contact lenses, and can also be used to quantitate CE from solutions and other materials. While *Fusarium spp.* was the focus in this study the method could easily be adapted to other fungal genera and species.

Spore surface hydrophobicity was increased in AFR4△*fmk1*. AFR4 spores were able to associate with a commercially available hydrogel lens 7x better than AFR4△*fmk1*. This change in association is likely due to the hydrophilic nature of the hydrogel contact lens (48) and the increased hydrophobicity seen with disruption of *fmk1*. It is likely that should this experiment be repeated using silicone hydrogel lenses, which tend to have hydrophobic surface properties, that an increase in association would be seen with AFR4△*fmk1*.

**FMK1 is Required for Chemotropism**

The ability to sense changes and respond to conditions in the environment is crucial to the survival of *F. solani*. Chemotaxis is the ability to move towards a stimulus, and chemotropism is growth directed towards a stimulus. *F. solani* utilizes chemotropism to detect and respond to a variety of stimuli in the environment such as nutrient concentrations and mating pheromones (2).

Since chemotropism is regulated by signal transduction cascades, the role of FMK1 in chemotropism of *F. solani* AFR4 was investigated. It was first hypothesized that germ tube emergence would be affected by inactivation of *fmk1*, but both the wild-type and mutant strain displayed random germination patterns. These random germination patterns observed in both strains indicate that FMK1 does not play a role in germ tube emergence.

A difference in hyphal growth patterns was observed following germ tube emergence. Wet weight measurements were used to determine growth rates for AFR4 and AFR4△*fmk1* to determine if the differences observed were due to growth rate or tactic behavior. The growth rate of AFR4△*fmk1* was identical to the wild-type. To investigate chemotropism, wild-type and mutant behavior were compared using percent growth towards nutrient as described above. The wild-type displayed directed growth towards the nutrient source while AFR4△*fmk1* displayed equal growth and stunted growth in all directions. This can be attributed to a disruption in the chemotropic cascade as the rate of growth was not affected in broth cultures.

Previous studies have indicated that infection of the root structure of plants is linked to MAP kinase cascades. The waxy covering of plant roots was hypothesized to be a nutrient barrier similar to the lens/eye model. To determine if chemotropism played a role in penetration of contact lenses, an eye/lens model was created using a fungal growth chamber. As seen in Figure 6, the wild-type is able to penetrate through the non-nutrient layer, representing the lens, towards the nutrient layer, representing the eye, while the mutant displays growth only near the surface of the lens layer. The mutant is able to penetrate through the lens layer and spiral shaped penetration is visible. The growth lacks direction in the mutant strain signifying a disruption in chemotropism due to the inactivation of *fmk1*.

**FMK1 is Required for Invasive Growth in Tissue**

MAP kinase is part of a highly conserved signal transduction cascade regulating various cellular responses. FMK1, one MAPK identified in *Fusarium*, is activated by phosphorylation of threonine and tyrosine residues located within the coding region (27). The MAP kinase signal transduction cascade allows the organism to sense changes in its environment and respond appropriately. Many organisms have multiple MAPK cascades. One such example is *Saccharomyces cerevisiae*. Five individual cascades are recognized within *S. cerevisiae* controlling mating, sporulation, filamentation, osmolarity response, and cell wall modeling (50). MAP kinases cascades typically consist of three kinases (MAPKKK, MAPKK, and MAPK) bound by scaffolding proteins (4). Activation of MAP kinase cascades results in the phosphorylation of regulatory proteins including transcription factors and other protein kinases (27). Inactivation of FMK1 by disruption of the TXY sequence by insertion of a $PLE^R$ cassette affected *F. solani* AFR4 growth in tissue. This MAP kinase has previously been shown to be necessary for invasive growth on plant tissue. (14).

Disruption of *fmk1* leads to a decrease in spore association with hydrogel contact lenses as well as to a disruption in chemotropism in an eye/lens model. To determine if an animal mitogen may increase penetration through hydrogel lenses, commercially available lenses were placed onto porcine eyes and inoculated. After 24 hours, AFR4 hyphal growth was detected on both sides of the lens without evidence of penetration. It was determined that water currents in and around the lens transported conidia and invalidated the experiment.

Rarely is a pathogen able to infect both animal and plant sources. *F. solani* was described as cross infective in 1980 when Cuero described a clinical isolate that was able to infect beans, corn and tomato plants (12, 35). Recently fusaria research has focused on

multilocus haplotyping. The aim of this multilocus haplotyping was to characterize the pathogenicity potential of over 45 strains of *F. solani*. The multilocus haplotyping is based on structural genes and places *F. solani* AFR4 into FSSC 1(1). All mycosis related species are designated FSSC 3 (40).

*F. solani* AFR4, a member of the FSSC 1 plant associated clade of the *Fusarium solani* species complex, grew invasively within animal tissues. The increase in invasive growth instigated the increase in global flaccidity observed in ocular tissue infected with AFR4. The difference in invasive tissue growth indicates that in both animal tissue, as well as laboratory media, FMK1 plays a role in nutrient sensing. Animal-based mitogens are sensed and the cell responds using the same signal transduction pathway involved in sensing plant and laboratory-based nutrients. Mechanisms of pathogenesis for *F. solani*, appear to be conserved.

Contact lenses served as the vehicle of transmission from the environment to the eye in the *Fusrium* keratitis outbreak occurring between 2004 and 2006. The role of MAP kinase, FMK1, was shown to have no role in the production of penetration pegs in nutrient agar as well as in silicone hydrogel lenses. AFR4 penetrated the lens with higher frequency but this is likely due to increased hyphal development and increased conidial association with the silicone hydrogel lens. Microconidia of AFR4△*fmk1* were unable to germinate in the PBS buffer and this could likely be cause for a decrease in hyphal mass as well as penetration. Penetration pegs were present in eye/lens models and on lenses for both strains AFR4 and AFR4△*fmk1*, indicating that FMK1 does not affect lens penetration.

For a pathogen to be effective it must be able to sense and quickly respond to its environment. A pathogen must first recognize a suitable host, FMK1 is essential in *F. oxysporum*, for pathogenicity in plants, and in this research the role of FMK1 in contact lens

associated *Fusarium* has been defined. FMK1 affects spore surface hydrophobicity which influences how the conidia associate with the lens polymer. The effect of FMK1 will vary with lens type, as lenses are constructed of varying polymers and subjected to variable surface treatments. FMK1 is also responsible for chemotropism towards laboratory and animal-based nutrients. For a pathogen to be effective it must first detect a suitable host, and then adapt its metabolism and morphology for pathology making chemotropism, thus *fmk1*, essential for pathogenesis. FMK1 has been described as essential for pathogenesis in plants and now in a human model. To increase the efficacy of multilocus haplotyping in predicting pathogenicity, it may be beneficial to include *fmk1* as a locus. While it is atypical for one species to be pathogenic of animals and plants, *Fusarium* are an exception. Cross-infectivity has been described from plant to animal and animal to plant. The current research demonstrates that pathogenicity pathways are likely conserved.

REFERENCES

1. **Ahearn, D. G., S. Zhang, R. D. Stulting, B. L. Schwam, R. B. Simmons, M. Ward, G. E. Pierce, and S. A. Crow, Jr.** Relative in vitro rates of attachment and penetration of hydrogel soft contact lenses by haplotypes of *Fusarium*. Cornea (In Press).

2. **Arkowitz, R. A.** 1999. Responding to attraction: chemotaxis and chemotropism in *Dictyostelium* and yeast. Trends Cell Biol **9:**20-7.

3. **Austwick, P.** 1984. *Fusarium* infections in man and animals, p. 129-140. *In* M. Moss and J. Smith (ed.), The applied mycology of *Fusarium*. Cambridge University Press, Cambridge.

4. **Bashor, C. J., N. C. Helman, S. Yan, and W. A. Lim.** 2008. Using engineered scaffold interactions to reshape MAP kinase pathway signaling dynamics. Science **319:**1539-43.

5. **Beattie, T. K., A. Tomlinson, and D. V. Seal.** 2003. Surface treatment or material characteristic: the reason for the high level of Acanthamoeba attachment to silicone hydrogel contact lenses. Eye Contact Lens **29:**S40-3; discussion S57-9, S192-4.

6. **Booth, C.** 1984. The *Fusarium* problem: historical, economic, and taxonomic aspects, p. 1-14. *In* M. Moss and J. Smith (ed.), The applied mycology of *Fusarium*. Cambridge University Press, Cambridge.

7. **Bowman, J. C., G. K. Abruzzo, J. W. Anderson, A. M. Flattery, C. J. Gill, V. B. Pikounis, D. M. Schmatz, P. A. Liberator, and C. M. Douglas.** 2001. Quantitative PCR assay to measure *Aspergillus fumigatus* burden in a murine model of disseminated aspergillosis: demonstration of efficacy of caspofungin acetate. Antimicrob Agents Chemother **45:**3474-81.

8. **Buffington, J. R., R. B. Simmons, L. A. Wilson, and D. G. Ahearn.** 1988. Effect of polymer differences on fungal penetration of hydrogel lenses. Journal of Industrial Microbiology **3:**29-32.

9. **Cai, X., K. M. Woods, S. J. Upton, and G. Zhu.** 2005. Application of quantitative real-time reverse transcription-PCR in assessing drug efficacy against the intracellular pathogen *Cryptosporidium parvum* in vitro. Antimicrob Agents Chemother **49:**4437-42.

10. **CDC** May 5 2006, posting date. *Fusarium* keratitis update. Media Relations. [Online.]

11. **Chang, D. C., G. B. Grant, K. O'Donnell, K. A. Wannemuehler, J. Noble-Wang, C. Y. Rao, L. M. Jacobson, C. S. Crowell, R. S. Sneed, F. M. T. Lewis, J. K. Schaffzin, M. A. Kainer, C. A. Genese, E. C. Alfonso, D. B. Jones, A. Srinivasan, S. K. Fridkin, and B. J. Park.** 2006. Multistate outbreak of *Fusarium* keratitis associated with use of a contact lens solution. Jama-Journal of the American Medical Association **296:**953-963.

12. **Cuero, R. G.** 1980. Ecological distribution of *Fusarium solani* and its opportunistic action related to mycotic keratitis in Cali, Colombia. J Clin Microbiol **12:**455-61.

13. **Dharmaraj, S.** 2007. RT-PCR: The Basics, Ambion.

14. **Di Pietro, A., F. I. Garcia-Maceira, E. Meglecz, and M. I. G. Roncero.** 2001. A MAP kinase of the vascular wilt fungus *Fusarium oxysporum* is essential for root penetration and pathogenesis. Molecular Microbiology **39:**1140-1152.

15. **Di Pietro, A., and M. I. Roncero.** 1998. Cloning, expression, and role in pathogenicity of pg1 encoding the major extracellular endopolygalacturonase of the vascular wilt pathogen *Fusarium oxysporum*. Mol Plant Microbe Interact **11:**91-8.

16. **Diaz, M.** 2006. Bead suspension arrays for identify fungal pathogens. Microbe **2:**74-81.

17. **Ferrer, C., J. Alio, A. Rodriguez, M. Andreu, and F. Colom.** 2005. Endophthalmitis caused by *Fusarium proliferatum*. J Clin Microbiol **43:**5372-5.

18. **Foroozan, R., R. Eagle, and E. Cohen.** 2000. Fungal keratitis in a soft contact lens wearer. CLAO Journal **26:**166-168.

19. **Geiser, D. M., M. D. Jimenez-Gasco, S. C. Kang, I. Makalowska, N. Veeraraghavan, T. J. Ward, N. Zhang, G. A. Kuldau, and K. O'Donnell.** 2004. FUSARIUM-ID v. 1.0: A DNA sequence database for identifying *Fusarium*. European Journal of Plant Pathology **110:**473-479.

20. **Glass, N. L., and G. C. Donaldson.** 1995. Development of primer sets designed for use with the PCR to amplify conserved genes from filamentous ascomycetes. Appl Environ Microbiol **61:**1323-30.

21. **Harrington, T. C., J. Steimel, F. Workneh, and X. B. Yang.** 2000. Molecular identification of fungi associated with vascular discoloration of soybean in the north central United States. Plant Disease **84:**83-89.

22. **Heitz, R., and J. Enoch.** 1987. Leonardo da Vinci: An assessment on his discourses on image formation in the eye, p. 19-26, Advances in Diagnostic Visual Optics. Springer-Verlag.

23. **Hennequin, C., E. Abachin, F. Symoens, V. Lavarde, C. Reboux, N. Nolard, and P. Berche.** 1999. Identification of *Fusarium* species involved in human infections by 28S rRNA gene sequencing. J Clin Microbiol **37:**3586-3589.

24. **Hoffmann, B., S. E. Eckert, S. Krappmann, and G. H. Braus.** 2001. Sexual diploids of *Aspergillus nidulans* do not form by random fusion of nuclei in the heterokaryon. Genetics **157:**141-7.

25. **Hue, F. X., M. Huerre, M. A. Rouffault, and C. de Bievre.** 1999. Specific detection of *Fusarium* species in blood and tissues by a PCR technique. J Clin Microbiol **37:**2434-2438.

26. **Jaeger, E. E., N. M. Carroll, S. Choudhury, A. A. Dunlop, H. M. Towler, M. M. Matheson, P. Adamson, N. Okhravi, and S. Lightman.** 2000. Rapid detection and identification of *Candida*, *Aspergillus*, and *Fusarium* species in ocular samples using nested PCR. J Clin Microbiol **38:**2902-8.

27. **Johnson, L. N., M. E. Noble, and D. J. Owen.** 1996. Active and inactive protein kinases: structural basis for regulation. Cell **85:**149-58.

28. **Jones, J., and B. Tighe.** 2004. Silicone Hydrogel Contact Lens Materials Update. Silicone Hydrogels **July**.

29. **Khor, W. B., T. Aung, S. M. Saw, T. Y. Wong, P. A. Tambyah, A. L. Tan, R. Beuerman, L. Lim, W. K. Chan, W. J. Heng, J. Lim, R. S. K. Loh, S. B. Lee, and D. T. H. Tan.** 2006. An outbreak of *Fusarium* keratitis associated with contact lens wear in Singapore. Jama-Journal of the American Medical Association **295:**2867-2873.

30. **Kim, Y. K., T. Kawano, D. Li, and P. E. Kolattukudy.** 2000. A mitogen-activated protein kinase kinase required for induction of cytokinesis and appressorium formation by host signals in the conidia of *Colletotrichum gloeosporioides*. Plant Cell **12:**1331-43.

31. **Kumar, S., J. Boehm, and J. C. Lee.** 2003. p38 MAP kinases: key signalling molecules as therapeutic targets for inflammatory diseases. Nat Rev Drug Discov **2:**717-26.

32. **Malardier, L., M. J. Daboussi, J. Julien, F. Roussel, C. Scazzocchio, and Y. Brygoo.** 1989. Cloning of the nitrate reductase gene (niaD) of Aspergillus nidulans and its use for transformation of *Fusarium oxysporum*. Gene **78:**147-56.

33. **Mandell, R.** 1988. Contact Lens Practice, 4 ed. Charles C. Thomas Springfield, IL.

34. **Marshall, C. J.** 1994. MAP kinase kinase kinase, MAP kinase kinase and MAP kinase. Curr Opin Genet Dev **4:**82-9.

35. **Mehl, H. L., and L. Epstein.** 2007. *Fusarium solani* species complex isolates conspecific with *Fusarium solani* f. sp. cucurbitae race 2 from naturally infected human and plant tissue and environmental sources are equally virulent on plants, grow at 37 degrees C and are interfertile. Environ Microbiol **9:**2189-99.

36. **Millar, B. C., X. Jiru, M. J. Walker, J. P. Evans, and J. E. Moore.** 2003. False identification of *Coccidioides immitis*: do molecular methods always get it right? J Clin Microbiol **41:**5778-5780.

37. **Miller, M., D. Callahan, D. McGrath, R. Manchester, and S. Norton.** 2001 Disinfection efficacy of contact lens care solutions against ocular pathogens. CLAO Journal **21:**16-22.

38. **Nelson, P. E., M. C. Dignani, and E. J. Anaissie.** 1994. Taxonomy, Biology, and Clinical Aspects of *Fusarium* Species. Clinical Microbiology Reviews **7:**479-&.

39. **Ninet, B., I. Jan, O. Bontems, Lechenne, O. Jousson, D. Lew, J. Schrenzel, R. G. Panizzon, and M. Monod.** 2005. Molecular identification of *Fusarium* species in onychomycoses. Dermatology **210:**21-25.

40. **O'Donnell, K., D. A. Sutton, A. Fothergill, D. McCarthy, M. G. Rinaldi, M. E. Brandt, N. Zhang, and D. M. Geiser.** 2008. Molecular phylogenetic diversity, multilocus haplotype nomenclature, and in vitro antifungal resistance within the *Fusarium solani* species complex. J Clin Microbiol **46:**2477-90.

41. **Ortoneda, M., J. Guarro, M. P. Madrid, Z. Caracuel, M. I. Roncero, E. Mayayo, and A. Di Pietro.** 2004. *Fusarium oxysporum* as a multihost model for the genetic dissection of fungal virulence in plants and mammals. Infect Immun **72:**1760-6.

42. **Page, W. J., and J. J. Stock.** 1971. Regulation and self-inhibition of *Microsporum gypseum* macroconidia germination. J Bacteriol **108:**276-81.

43. **Rabilloud, T., V. Brodard, G. Peltre, P. G. Righetti, and C. Ettori.** 1992. Modified silver staining for immobilized pH gradients. Electrophoresis **13:**264-6.

44. **Reischer, G. H., M. Lemmens, A. Farnleitner, A. Adler, and R. L. Mach.** 2004. Quantification of *Fusarium graminearum* in infected wheat by species specific real-time PCR applying a TaqMan Probe. J Microbiol Methods **59:**141-6.

45. **Ren, P., D. G. Ahearn, and S. A. Crow, Jr.** 1999. Comparative study of *Aspergillus mycotoxin* production on enriched media and construction material. J Ind Microbiol Biotechnol **23:**209-13.

46. **Robinson, P. M.** 1973. Oxygen-positive chemotropic factor for fungi. New Phytol. **72:**1349-56.

47. **Rosenthal, R., N. Dassanayake, R. Schlitzer, B. Schlech, D. Meadows, and R. Stone.** 2006. Biocide uptake in contact lenses and loss of fungicidal activity during storage of contact lenses. Eye and Contact Lens **32:**262-266.

48. **Santos, L., D. Rodrigues, M. Lira, M. E. Oliveira, R. Oliveira, E. Y. Vilar, and J. Azeredo.** 2007. The influence of surface treatment on hydrophobicity, protein adsorption and microbial colonisation of silicone hydrogel contact lenses. Cont Lens Anterior Eye **30:**183-8.

49. **Schaad, N. W., and R. D. Frederick.** 2002. Real-time PCR and its application for rapid plant disease diagnostics. Canadian Journal of Plant Pathology-Revue Canadienne De Phytopathologie **24:**250-258.

50. **Schaeffer, H. J., and M. J. Weber.** 1999. Mitogen-activated protein kinases: specific messages from ubiquitous messengers. Mol Cell Biol **19:**2435-44.

51. **Schweigkofler, W., K. O'Donnell, and M. Garbelotto.** 2004. Detection and quantification of airborne conidia of *Fusarium circinatum*, the causal agent of pine pitch canker, from two California sites by using a real-time PCR approach combined with a simple spore trapping method. Appl Environ Microb **70:**3512-3520.

52. **Snyder, C.** 2006. Lens care complications--where's the rub? Contact lens and Anterior Eye **29:**161-162.

53. **Stone, R.** 1988. Why Contact Lens Groups?, p. 38-41, *Contact Lens Spectrum*, vol. 3.

54. **Van Burik, J. A., D. Myerson, R. W. Schreckhise, and R. A. Bowden.** 1998. Panfungal PCR assay for detection of fungal infection in human blood specimens. J Clin Microbiol **36:**1169-1175.

55. **Zegans, M. E., H. I. Becker, J. Budzik, and G. O'Toole.** 2002. The role of bacterial biofilms in ocular infections. DNA Cell Biol **21:**415-20.

56. **Zhang, N., K. O'Donnell, D. A. Sutton, F. A. Nalim, R. C. Summerbell, A. A. Padhye, and D. M. Geiser.** 2006. Members of the *Fusarium solani* species complex that cause infections in both humans and plants are common in the environment. J Clin Microbiol **44:**2186-2190.

57. **Zhang, S., D. G. Ahearn, J. A. Noble-Wang, R. D. Stulting, B. L. Schwam, R. B. Simmons, G. E. Pierce, and S. A. Crow, Jr.** 2006. Growth and survival of *Fusarium*

*solani-F. oxysporum* complex on stressed multipurpose contact lens care solution films on plastic surfaces in situ and in vitro. Cornea **25:**1210-6.